

Effective connections of a_μ , Higgs physics, and the collider frontier

Anisha,^{1,*} Upalaparna Banerjee^{1,†}, Joydeep Chakraborty,^{1,‡} Christoph Englert,^{2,§}
Michael Spannowsky,^{3,||} and Panagiotis Stylianou^{2,¶}

¹Indian Institute of Technology Kanpur, Kalyanpur, Kanpur 208016, India

²School of Physics and Astronomy, University of Glasgow, Glasgow G12 8QQ, United Kingdom

³Institute for Particle Physics Phenomenology, Durham University, Durham DH1 3LE, United Kingdom



(Received 27 August 2021; accepted 11 December 2021; published 24 January 2022)

We consider scalar extensions of the Standard Model (SM) and their effective field theoretic generalizations to illustrate the phenomenological connection between precision measurements of the anomalous magnetic moment of the muon a_μ , precision Higgs measurements, and direct collider sensitivity. To this end, we consider charged beyond Standard Model (BSM) scalar sectors of the Zee-Babu type for which we develop a consistent and complete dimension-5 and -6 effective field theory extensions. This enables us to track generic new physics effects that interact with the SM predominantly via radiative interactions. While the operator space is high dimensional, the intersection of exotics searches at the Large Hadron Collider (LHC), Higgs signal strength, and anomalous muon magnetic measurements is manageably small. We find that consistency of LHC Higgs observations and a_μ requires a significant deformation of the new states' electroweak properties. Evidence in searches for doubly charged scalars as currently pursued by the LHC experiments can be used to further tension the BSMEFT parameter space and resolve blind directions in the effective field theory (EFT)-extended Zee-Babu scenario.

DOI: [10.1103/PhysRevD.105.016019](https://doi.org/10.1103/PhysRevD.105.016019)

I. INTRODUCTION

The search for new physics beyond the Standard Model (SM), albeit so far unsuccessful at the Large Hadron Collider (LHC), is key to the current particle physics phenomenology program. The recent measurement of the anomalous muon magnetic moment,

$$a_\mu = \frac{(g-2)_\mu}{2}, \quad (1)$$

at Fermilab [1] aligns with the previous results obtained at the BNL E821 experiment [2], leading to a $\sim 4\sigma$ discrepancy [3–22] (see also [23]),

$$\Delta a_\mu = a_\mu(\text{exp}) - a_\mu(\text{SM}) = (25.1 \pm 5.9) \times 10^{-10}. \quad (2)$$

*anisha@iitk.ac.in

†upalab@iitk.ac.in

‡joydeep@iitk.ac.in

§christoph.englert@glasgow.ac.uk

||michael.spannowsky@durham.ac.uk

¶p.stylianou.1@research.gla.ac.uk

Published by the American Physical Society under the terms of the [Creative Commons Attribution 4.0 International license](https://creativecommons.org/licenses/by/4.0/). Further distribution of this work must maintain attribution to the author(s) and the published article's title, journal citation, and DOI. Funded by SCOAP³.

While this deviation is a long standing and potentially tantalizing hint for the existence of new interactions beyond the SM that deserves further scrutiny from all angles (see, e.g., [24]), it is flanked by broad consistency of collider measurements with the SM. In particular, this includes an increasing statistical control in searches for new heavy beyond Standard Model (BSM) states and an enhanced precision in BSM tell-tale modifications of, e.g., precision Higgs data.

On the one hand, one interpretation of this result is a large scale separation between the SM and BSM interactions, perhaps in the range $\Lambda \gtrsim 10$ TeV [25–33]. On the other hand, such tight constraints on the scale of new physics, while being bad news for the ongoing collider program, are very much a statement of model-specific correlations, which can be consistently modified by employing effective field theory (EFT) techniques. This is the purpose of this work: we perform a case study of the interplay of Higgs precision physics, a_μ , and direct LHC sensitivity for the Zee-Babu model [34–36], extended by effective interactions. The Zee-Babu model is the simplest framework containing new exotic states (singly and a doubly charged scalars) that also address open questions in neutrino physics. It is known that the Zee-Babu extension leads to a negative contribution to the anomalous magnetic moment [37–40]. At face value, this means that this scenario is under pressure by the anomalous magnetic moment measurement. However, when supplied with

additional effective interaction related momentum enhancements that predominantly communicate with the scalar sector extension, it could, in principle, address this shortcoming and thereby resurrect the model's many theoretically appealing implications. In parallel, we demonstrate that the EFT extension of the Zee-Babu model becomes particularly transparent when we connect a_μ with available Higgs data constraints and direct search strategies for exotic states. This motivates the considered Zee-Babu extension as an interesting candidate theory to study the phenomenology across the precision and high energy frontiers in the future (see also [41]).

We note that our approach extends earlier, purely SMEFT [42] investigations (see, e.g., [43]) by reintroducing a model-specific angle. In the SMEFT context, the attained precision of a_μ can push correlated new physics constraints into the PeV regime [44], rendering the present and any future collider physics program largely blind to the dynamics of Δa_μ . Addressing cancellations at low scales (i.e., the muon mass) by means of deformed interactions of new states that fall into the kinematic coverage of the LHC allows us to phenomenologically generalize the SMEFT-based findings and further motivate searches for, e.g., doubly charged scalars in the future.¹

This work is organized as follows: In Sec. II, we briefly review the Zee-Babu model before providing a detailed discussion of its dimension-5 and -6 EFT extensions. In Sec. III, we turn to the phenomenological implications that we focus on in this paper, i.e., the anomalous muon magnetic moment in Sec. III A, expected modifications of 125 GeV Higgs boson measurements in Sec. III B, and the direct sensitivity to doubly charged scalar bosons as a smoking gun of this scenario in Sec. III C. In Sec. IV, we combined these three searches to highlight their complementarity and intersection. We conclude in Sec. V.

II. THE MODEL

The Zee-Babu model [34,35] is an extension of the usual SM Lagrangian by two $SU(2)_L$ and color singlet scalar fields with nontrivial hypercharges,

$$\begin{aligned} \mathcal{S} &: (\mathbf{1}, \mathbf{1}, 1), \\ \mathcal{R} &: (\mathbf{1}, \mathbf{1}, 2). \end{aligned} \quad (3)$$

These give rise to the new renormalizable and effective interactions determined by the gauge symmetry $SU(3)_C \otimes SU(2)_L \otimes U(1)_Y$. The renormalizable Lagrangian is given by

¹Naturally, our findings are then specific to the EFT extension of the considered Zee-Babu scenario. We leave an analysis of all scalar extensions (or even beyond that) for future work.

$$\begin{aligned} \mathcal{L}_{\text{renorm}} = & -\frac{1}{4}G_{\mu\nu}^A G^{A\mu\nu} - \frac{1}{4}W_{\mu\nu}^I W^{I\mu\nu} - \frac{1}{4}B_{\mu\nu} B^{\mu\nu} \\ & + (\mathcal{D}_\mu \phi)^\dagger (\mathcal{D}^\mu \phi) + (\mathcal{D}_\mu \mathcal{S})^\dagger (\mathcal{D}^\mu \mathcal{S}) + (\mathcal{D}_\mu \mathcal{R})^\dagger (\mathcal{D}^\mu \mathcal{R}) \\ & - \mathcal{V}(\phi, \mathcal{S}, \mathcal{R}) + i(\bar{L}\gamma^\mu \mathcal{D}_\mu L + \bar{e}\gamma^\mu \mathcal{D}_\mu e + \bar{Q}\gamma^\mu \mathcal{D}_\mu Q \\ & + \bar{u}\gamma^\mu \mathcal{D}_\mu u + \bar{d}\gamma^\mu \mathcal{D}_\mu d) + (\mathcal{L}_{\text{Yukawa}} + \text{H.c.}), \end{aligned} \quad (4)$$

where

$$\begin{aligned} G_{\mu\nu}^A &= \partial_\mu G_\nu^A - \partial_\nu G_\mu^A + g_3 f^{ABC} G_\mu^B G_\nu^C, \\ W_{\mu\nu}^I &= \partial_\mu W_\nu^I - \partial_\nu W_\mu^I + g e^{IJK} W_\mu^J W_\nu^K, \\ B_{\mu\nu} &= \partial_\mu B_\nu - \partial_\nu B_\mu, \end{aligned} \quad (5)$$

are the field strength tensors corresponding to $SU(3)_C$, $SU(2)_L$, and $U(1)_Y$, respectively, and here $\{A, B, C\} \in \{1, 2, \dots, 8\}$, and $\{I, J, K\} \in \{1, 2, 3\}$.

The scalar potential $\mathcal{V}(\phi, \mathcal{S}, \mathcal{R})$ in Eq. (3) reads

$$\begin{aligned} \mathcal{V}(\phi, \mathcal{S}, \mathcal{R}) = & \mu_1^2 (\phi^\dagger \phi) + \mu_2^2 (\mathcal{S}^\dagger \mathcal{S}) + \mu_3^2 (\mathcal{R}^\dagger \mathcal{R}) \\ & + m (\mathcal{S}^2 \mathcal{R}^\dagger + (\mathcal{S}^\dagger)^2 \mathcal{R}) + \lambda_1 (\phi^\dagger \phi)^2 \\ & + \lambda_2 (\mathcal{S}^\dagger \mathcal{S})^2 + \lambda_3 (\mathcal{R}^\dagger \mathcal{R})^2 \\ & + \lambda_4 (\phi^\dagger \phi) (\mathcal{S}^\dagger \mathcal{S}) + \lambda_5 (\phi^\dagger \phi) (\mathcal{R}^\dagger \mathcal{R}) \\ & + \lambda_6 (\mathcal{S}^\dagger \mathcal{S}) (\mathcal{R}^\dagger \mathcal{R}). \end{aligned} \quad (6)$$

In contrast to the SM, the quantum numbers of the Zee-Babu singlet scalars allow new quartic as well as trilinear interactions, as can be seen in Eq. (6). We have denoted the new quartic couplings as $\lambda_2, \lambda_3, \lambda_4, \lambda_5$, and λ_6 , whereas m parametrizes the trilinear scalar interaction.

$\mathcal{L}_{\text{Yukawa}}$ contains two new Yukawa-like interactions along with the usual SM ones,

$$\begin{aligned} \mathcal{L}_{\text{Yukawa}} = & -y_e \bar{L} e \phi - y_u \bar{Q} u \tilde{\phi} - y_d \bar{Q} d \phi \\ & - f_S (\bar{L}^c i \tau_2 L) \mathcal{S} - f_R (\bar{e}^c e) \mathcal{R}. \end{aligned} \quad (7)$$

Here, $\tilde{\phi}_i = \epsilon_{ij} \phi_j^*$ is the charge-conjugated Higgs doublet. The Yukawa couplings f_S and f_R parametrize the interactions between $SU(2)_L$ lepton doublet L , singlet e with scalars \mathcal{S} , and \mathcal{R} , respectively.

Bounds on the parameters in Eq. (6) can be derived from examining the shape of $\mathcal{V}(\phi, \mathcal{S}, \mathcal{R})$. For the potential to be bounded from below, each of λ_1, λ_2 , and λ_3 should be positive. To achieve the overall positivity of the potential, one can find the following relations, see e.g., [45]:

$$\begin{aligned} \lambda_4/2\sqrt{\lambda_1\lambda_2} &> -1, & \lambda_5/2\sqrt{\lambda_1\lambda_3} &> -1, \\ \lambda_6/2\sqrt{\lambda_2\lambda_3} &> -1. \end{aligned} \quad (8)$$

Apart from that, there are $\sim 4\pi$ perturbativity bounds for λ_i , $i = 2, \dots, 6$.

After electroweak symmetry breaking, ϕ acquires a vacuum expectation value (vev) and gives rise to the

TABLE I. Explicit structures of the dimension-5 and -6 operators contributing to muon anomalous magnetic moment, loop-induced Higgs decay, and production and decay for h^\pm and $r^{\pm\pm}$. The operators in bold have distinct Hermitian conjugates: $A \in \{1, 2, \dots, 8\}$ and $I \in \{1, 2, 3\}$.

Φ^5		$\Psi^2\Phi^2$	
\mathcal{O}_r	$(\phi^\dagger\phi)\mathcal{R}^\dagger\mathcal{S}^2$	$\mathcal{O}_{le\phi\mathcal{S}}$	$\bar{L}e\tilde{\phi}\mathcal{S}$
$\Phi^4\mathcal{D}^2$		Φ^6	
$\mathcal{O}_{\phi\mathcal{R}\mathcal{D}}$	$(\phi^\dagger\phi)[(\mathcal{D}^\mu\mathcal{R})^\dagger(\mathcal{D}_\mu\mathcal{R})]$	$\mathcal{O}_{\phi\mathcal{R}}$	$(\phi^\dagger\phi)^2(\mathcal{R}^\dagger\mathcal{R})$
$\mathcal{O}_{\phi\mathcal{S}\mathcal{D}}$	$(\phi^\dagger\phi)[(\mathcal{D}^\mu\mathcal{S})^\dagger(\mathcal{D}_\mu\mathcal{S})]$	$\mathcal{O}_{\phi\mathcal{S}}$	$(\phi^\dagger\phi)^2(\mathcal{S}^\dagger\mathcal{S})$
$\mathcal{O}_{\mathcal{R}\phi\mathcal{D}}$	$(\mathcal{R}^\dagger\mathcal{R})[(\mathcal{D}^\mu\phi)^\dagger(\mathcal{D}_\mu\phi)]$		
$\mathcal{O}_{\mathcal{S}\phi\mathcal{D}}$	$(\mathcal{S}^\dagger\mathcal{S})[(\mathcal{D}^\mu\phi)^\dagger(\mathcal{D}_\mu\phi)]$		
$\Psi^2\Phi^2\mathcal{D}$		$\Psi^2\Phi^3$	
$\mathcal{O}_{\mathcal{R}le}$	$(\bar{L}^c\gamma^\mu e)(\phi i\mathcal{D}_\mu\mathcal{R})$	$\mathcal{O}_{l\phi\mathcal{S}}$	$(\bar{L}^c i\tau_2 L)(\phi^\dagger\phi)\mathcal{S}$
\mathcal{O}_{Sle}	$(\bar{L}^c\gamma^\mu e)(\tilde{\phi} i\mathcal{D}_\mu\mathcal{S})$	$\mathcal{O}_{l\phi\mathcal{R}}$	$(\bar{L}^c i\tau_2 L)(\phi^\dagger\mathcal{R}\tilde{\phi})$
$\mathcal{O}_{\mathcal{R}q}$	$(\bar{Q}\gamma^\mu Q)(\mathcal{R}^\dagger i\overleftrightarrow{\mathcal{D}}_\mu\mathcal{R})$	$\mathcal{O}_{e\mathcal{R}\phi}$	$(\phi^\dagger\phi)\mathcal{R}(e^c e)$
\mathcal{O}_{Sq}	$(\bar{Q}\gamma^\mu Q)(\mathcal{S}^\dagger i\overleftrightarrow{\mathcal{D}}_\mu\mathcal{S})$	$\mathcal{O}_{u\phi\mathcal{R}}$	$(\bar{Q}u)\tilde{\phi}(\mathcal{R}^\dagger\mathcal{R})$
$\mathcal{O}_{\mathcal{R}u}$	$(\bar{u}\gamma^\mu u)(\mathcal{R}^\dagger i\overleftrightarrow{\mathcal{D}}_\mu\mathcal{R})$	$\mathcal{O}_{u\phi\mathcal{S}}$	$(\bar{Q}u)\tilde{\phi}(\mathcal{S}^\dagger\mathcal{S})$
\mathcal{O}_{Su}	$(\bar{u}\gamma^\mu u)(\mathcal{S}^\dagger i\overleftrightarrow{\mathcal{D}}_\mu\mathcal{S})$		
$\Phi^2\chi^2$			
\mathcal{O}_{BR}	$B_{\mu\nu}B^{\mu\nu}(\mathcal{R}^\dagger\mathcal{R})$	$\mathcal{O}_{\bar{B}\mathcal{R}}$	$\bar{B}_{\mu\nu}B^{\mu\nu}(\mathcal{R}^\dagger\mathcal{R})$
\mathcal{O}_{BS}	$B_{\mu\nu}B^{\mu\nu}(\mathcal{S}^\dagger\mathcal{S})$	$\mathcal{O}_{\bar{B}\mathcal{S}}$	$\bar{B}_{\mu\nu}B^{\mu\nu}(\mathcal{S}^\dagger\mathcal{S})$
$\mathcal{O}_{W\mathcal{R}}$	$W_{\mu\nu}^I W^{I\mu\nu}(\mathcal{R}^\dagger\mathcal{R})$	$\mathcal{O}_{\bar{W}\mathcal{R}}$	$\bar{W}_{\mu\nu}^I W^{I\mu\nu}(\mathcal{R}^\dagger\mathcal{R})$
\mathcal{O}_{WS}	$W_{\mu\nu}^I W^{I\mu\nu}(\mathcal{S}^\dagger\mathcal{S})$	$\mathcal{O}_{\bar{W}\mathcal{S}}$	$\bar{W}_{\mu\nu}^I W^{I\mu\nu}(\mathcal{S}^\dagger\mathcal{S})$
\mathcal{O}_{GR}	$G_{\mu\nu}^A G^{A\mu\nu}(\mathcal{R}^\dagger\mathcal{R})$	$\mathcal{O}_{\bar{G}\mathcal{R}}$	$\bar{G}_{\mu\nu}^A G^{A\mu\nu}(\mathcal{R}^\dagger\mathcal{R})$
\mathcal{O}_{GS}	$G_{\mu\nu}^A G^{A\mu\nu}(\mathcal{S}^\dagger\mathcal{S})$	$\mathcal{O}_{\bar{G}\mathcal{S}}$	$\bar{G}_{\mu\nu}^A G^{A\mu\nu}(\mathcal{S}^\dagger\mathcal{S})$
$\Psi^2\Phi\chi$			
\mathcal{O}_{eBS}	$B_{\mu\nu}(\bar{L}^c\sigma^{\mu\nu}L)\mathcal{S}$	\mathcal{O}_{eWS}	$W_{\mu\nu}^I(\bar{L}^c\tau^I\sigma^{\mu\nu}L)\mathcal{S}$

physical Higgs H . \mathcal{S} and \mathcal{R} emerge as singly and doubly charged scalars h^\pm and $r^{\pm\pm}$, respectively.

We aim to track the generic physics that predominantly couples to \mathcal{S} , \mathcal{R} . To this end, we modify SM correlations not only through the presence of h^\pm and $r^{\pm\pm}$, but also through the interactions that arise from integrating out the new physics that further deform the \mathcal{S} , \mathcal{R} interactions with SM matter. We therefore extend the renormalizable Lagrangian with a complete, independent, and exhaustive set of dimension-5 and -6 effective operators,

$$\mathcal{L} = \mathcal{L}_{\text{renorm}} + \sum_{j=1}^N \frac{\mathcal{C}_j^{(5)}}{\Lambda} \mathcal{O}_j^{(5)} + \sum_{k=1}^M \frac{\mathcal{C}_k^{(6)}}{\Lambda^2} \mathcal{O}_k^{(6)}. \quad (9)$$

We choose to express the operator sets using the Warsaw basis methodology [42] (see also [46]). The complete set of effective operators that couple \mathcal{S} and \mathcal{R} to the SM fields

TABLE II. The renormalizable couplings and the singly and doubly charged scalar related operators that contribute to the muon anomalous magnetic moment.

Charged scalar type	Renormalizable couplings	Contributing operators
h^\pm	f_S	$\mathcal{O}_{\phi\mathcal{S}\mathcal{D}}$, \mathcal{O}_{eWS} , \mathcal{O}_{eBS} , \mathcal{O}_{Sle} , $\mathcal{O}_{l\phi\mathcal{S}}$.
$r^{\pm\pm}$	$f_{\mathcal{R}}$	$\mathcal{O}_{\phi\mathcal{R}\mathcal{D}}$, $\mathcal{O}_{e\mathcal{R}\phi}$, $\mathcal{O}_{\mathcal{R}le}$, $\mathcal{O}_{l\phi\mathcal{R}}$.

have been listed in Appendix A. For the purpose of our work, we consider only those operators that affect the anomalous magnetic moment for muons, the loop-induced neutral Higgs decays, and production and decay of the charged scalars. The gauge invariant structures for these operators are given in Table I. Throughout this paper, we consider real values for the Wilson coefficients (\mathcal{C}_k) alongside a trivial flavor structure of the new interactions.²

III. PHENOMENOLOGY

A. Muon anomalous magnetic moment

We first calculate the anomalous magnetic moment for muons for the considered scenario, extending well-documented results [37–40] to effective interactions. In Table II, we have listed the parameters and the operators contributing to a_μ .

The phenomenological appeal of a_μ is rooted in the fact that it provides an unambiguous BSM effect for UV-complete scenarios; when matching the contribution of a concrete BSM theory to the SMEFT operators that gives rise to a_μ (we refer the muon mass as M_μ),

$$\Delta a_{\text{SMEFT}} = \frac{\sqrt{2}vM_\mu}{e} \mathcal{C}_{eA}$$

$$= \frac{\sqrt{2}vM_\mu}{e} (\mathcal{C}_{eW} \sin\theta_W - \mathcal{C}_{eB} \cos\theta_W), \quad (10)$$

where the Wilson coefficients \mathcal{C}_{eW} , \mathcal{C}_{eB} of the operators \mathcal{O}_{eW} and \mathcal{O}_{eB} in the language of Refs. [42,47,48] are

$$\mathcal{O}_{eW} = W_{\mu\nu}^I (\bar{L}\sigma^{\mu\nu}e)\tau^I\phi,$$

$$\mathcal{O}_{eB} = B_{\mu\nu} (\bar{L}\sigma^{\mu\nu}e)\phi, \quad (11)$$

and ($\sigma^{\mu\nu} = i[\gamma^\mu, \gamma^\nu]/2$) will remain finite to all orders in perturbation theory. For the EFT model discussed in the above section, this remains true to one-loop order for a range of interactions, but broadly speaking, EFT insertions related to the SM or BSM particle content will generically imply a renormalization of the operators related to a_μ as well. This means that a_μ becomes a scheme-dependent

² $f_{\mathcal{R}}$ and f_S symmetric and antisymmetric couplings in lepton flavor space which project out these related combinations of Wilson coefficients in concrete calculations.

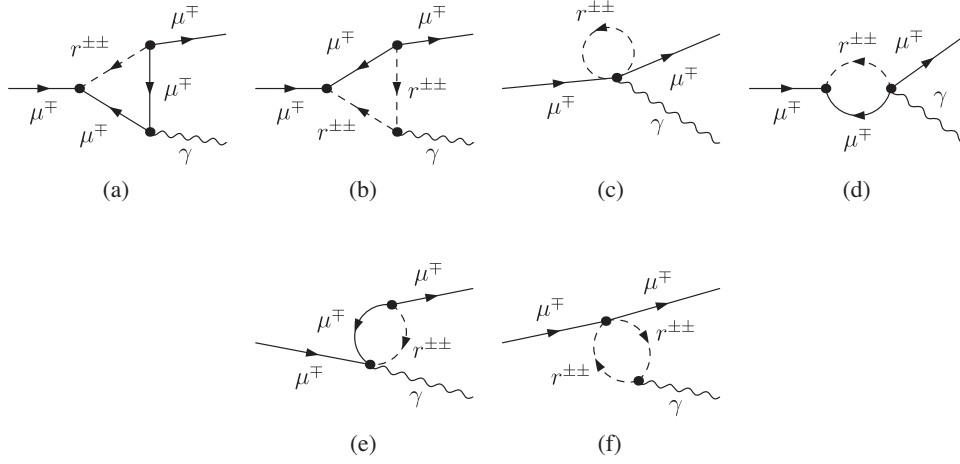


FIG. 1. BSM Feynman diagrams contributing to the muon anomalous magnetic moment $\mu \rightarrow \mu\gamma$ via the new propagating $r^{\pm\pm}$ and its EFT interactions. The vertices include the renormalizable and the dimension-6 interactions. Similar diagrams arise from the h^\pm scalar.

parameter rather than a UV-finite prediction (as in renormalizable models), and the precision of the obtained measurements of a_μ then motivates the inclusion of this observable to the defining input of the field theory (analogous to the Fermi constant in the electroweak SM). The precision of a_μ can then be used to tension predictions of observable measurements (we focus on Higgs and direct production in this work). In the following, we work in the mass basis of the SM as indicated in Eq. (10), where we consider $\mathcal{O}_{eA} = A_{\mu\nu}(\bar{e}\sigma^{\mu\nu}e)v$ (where $A_{\mu\nu}$ is the QED field strength).³

Concretely, we evaluate the one-loop three-point vertex function,

$$\Gamma^\mu = -ie\bar{u}(p') \left[\gamma^\mu F_1(k^2) + \frac{i}{2M_\mu} \sigma^{\mu\nu} k_\nu F_2(k^2) + \dots \right] u(p), \quad (12)$$

with momentum transfer $k = p' - p$. The ellipses denote additional form factors that appear in chiral gauge theories, e.g., the anomalous electric dipole moment. In this work, we limit ourselves to the anomalous magnetic moment,

$$a_\mu = F_2(0), \quad (13)$$

which is directly related to the effective Lagrangian of Eq. (9). We employ dimensional regularization and choose $\overline{\text{MS}}$ renormalization for the Wilson coefficients and on-shell renormalization for the remaining electroweak

³Renormalization of $Z - A$ mixing [49,50] implies the requirement of considering the Z boson-associated magnetic moment of the muon \mathcal{O}_{eZ} . In this work, however, we focus on a_μ , which means that the renormalization procedure is confined to \mathcal{C}_{eA} operator structures.

contributions, in particular, for the external muon fields (see [49] for a review); Feynman diagram contributions are shown in Fig. 1. When using one-loop EFT insertions, the implicit assumption is that any new degrees of freedom responsible for these interactions have been integrated out, and we consider terms up to $\sim 1/\Lambda^2$ (i.e., we truncate the series expansion at dimension-6 level) in this expansion. This enables us to renormalize the structure in Eq. (10) to cancel the divergence associated with the \mathcal{C}_{eA} Lorentz structure (details are presented in Appendix B). At the considered one-loop, Λ^{-2} level, these are exclusively given by the effective operator insertions related to h^\pm ; the dimension-6 singularities of a_μ arise from $\sim \mathcal{C}_{eBS}, \mathcal{C}_{eWS}$ loop contributions. We use FeynArts [51] to enumerate the relevant one-loop diagrams and FormCalc [52] for calculating the amplitudes and extracting the relevant form factor. PackageX [53] is used for simplifications of Passarino-Veltman scalar loop integrals [54].

The anomalous magnetic moment in the context of the Zee-Babu model has been studied extensively in the past (see, for example, Refs. [37–40]). We reproduce the standard result,

$$a_\mu^{\text{d4}}(\text{Zee-Babu}) = -\frac{M_\mu^2}{24\pi^2} \left(\frac{(f_S^\dagger f_S)_{\mu\mu}}{M_{h^\pm}^2} + 4 \frac{(f_{\mathcal{R}}^\dagger f_{\mathcal{R}})_{\mu\mu}}{M_{r^{\pm\pm}}^2} \right), \quad (14)$$

and the famous Schwinger result $\Delta a_\mu(\text{QED}) = \alpha/2\pi$ [55] as a cross check and to align conventions. A summary of the impact of EFT operators, alongside the sensitivity to renormalizable couplings of the scenario introduced in Sec. II is provided in Table II. The effect of different parameters on a_μ arising from the BSM contributions is shown in Fig. 2.

The contributions from the renormalizable charged scalar interactions are negative, Eq. (14), which is also clearly visible from Figs. 2(a)–2(c). To explain the

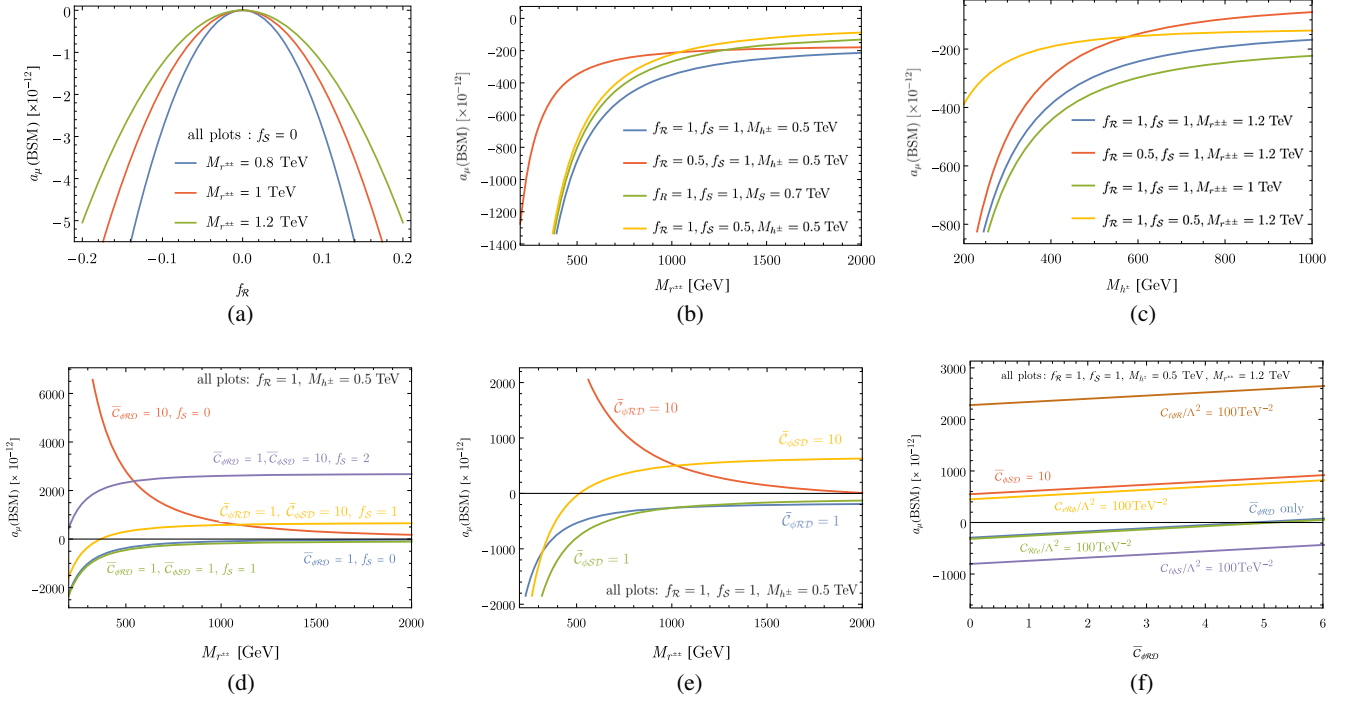


FIG. 2. Impact of various new physics parameters on a_μ (BSM). The top row shows the dependence on terms from the renormalizable part of the Lagrangian Eq. (4), while the bottom row includes effects from different effective operators. In (d), we investigate how large $\mathcal{C}_{\phi\mathcal{R}D}$ is required to be in order to get a positive result when only the doubly charged state is present, and we also show that $\mathcal{C}_{\phi\mathcal{R}D}$ can be kept low by introducing the singly charged scalar effective interactions through $\mathcal{C}_{\phi\mathcal{S}D}$. The effect of different values considered for each of $\mathcal{C}_{\phi\mathcal{R}D}$ and $\mathcal{C}_{\phi\mathcal{S}D}$ is shown in (e) when both scalars are included to probe how large each of these should be needed to generate a positive contribution. Panel (f) shows the linear dependence of the anomalous magnetic moment on $\mathcal{C}_{\phi\mathcal{R}D}$ and how it is shifted when introducing additional operators (we choose $\tilde{C}_i = C_i v^2/\Lambda^2$ for convenience).

experimental measurement of the anomalous magnetic moment, which favors a positive Δa_μ (BSM) slightly larger than the SM expectation, this negative contribution needs to be overcome by additional EFT contributions.

These can be logarithmically enhanced for large mass gaps $M_{r^{\pm\pm}}, M_{h^\pm} \gg M_\mu$. The a_μ contributions for the effective interactions related to $r^{\pm\pm}$ take a particularly compact form in the limit $M_{r^{\pm\pm}} \gg M_\mu$,

$$\Lambda^2 \times a_\mu^{\text{d6}, r^{\pm\pm}} (\text{Zee-Babu}) = \frac{f_{\mathcal{R}} M_\mu^2 v^2 (\mathcal{C}_{e\mathcal{R}\phi})_{\mu\mu}}{6\pi^2 M_{r^{\pm\pm}}^2} + \frac{f_{\mathcal{R}} M_\mu^2 v^2 (\mathcal{C}_{\ell\phi\mathcal{R}})_{\mu\mu}}{2\pi^2 M_{r^{\pm\pm}}^2} \left(\log\left(\frac{M_{r^{\pm\pm}}}{M_\mu}\right) - \frac{1}{4} \right) + \frac{f_{\mathcal{R}} M_\mu^3 v (\mathcal{C}_{\mathcal{R}\ell e})_{\mu\mu}}{\sqrt{2}\pi^2 M_{r^{\pm\pm}}^2} \left(\frac{7}{12} - \log\left(\frac{M_{r^{\pm\pm}}}{M_\mu}\right) \right) + \frac{f_{\mathcal{R}}^2 M_\mu^2 v^2 \mathcal{C}_{\phi\mathcal{R}D}}{12\pi^2 M_{r^{\pm\pm}}^2}. \quad (15)$$

This together with the fully renormalized h^\pm interactions give rise to the behavior shown Figs. 2(d)–2(f).⁴ In Fig. 2(f), it is clearly visible that a_μ (BSM) receives the dominant contribution from $\mathcal{C}_{\ell\phi\mathcal{R}}$. Besides, a sizable value chosen for $\mathcal{C}_{e\mathcal{R}\phi}$ or h^\pm interactions parameterized through $\mathcal{C}_{\phi\mathcal{S}D}$ can also be equally effective in generating a positive

a_μ (BSM). We have provided the contribution to a_μ (BSM) arising from h^\pm effective interactions in Appendix C.

The covariant structures of the operators $\mathcal{O}_{\phi\mathcal{R}D}$ and $\mathcal{O}_{\phi\mathcal{S}D}$, given in Table I, call for the redefinition of the charged scalar fields and as a consequence modify existing renormalizable charged scalar interaction vertices; thus, the corresponding Wilson coefficients $\mathcal{C}_{\phi\mathcal{R}D}$ and $\mathcal{C}_{\phi\mathcal{S}D}$ naturally provide a significant contribution to the observables. We investigate the ability of these Wilson coefficients to produce a reasonable positive a_μ (BSM) in Figs. 2(d) and 2(e).

⁴It is worth highlighting that these distributions include the Yukawa interactions of r^\pm, h^\pm , which means that there are nonvanishing BSM contributions to a_μ in all displayed cases.

Attributing the observed a_μ to either $\mathcal{C}_{\phi\mathcal{R}D}$ or $\mathcal{C}_{\phi\mathcal{S}D}$ related terms given in Eqs. (15) and (C1), respectively, requires large values for the Wilson coefficients, and we discuss the phenomenological implication of such a scenario below. In parallel, when we consider the contributions related to h^\pm , the observed $\mathcal{C}_{\phi\mathcal{R}D} - a_\mu$ correlation can be altered which again leads to experimentally testable implications (see Sec. IV).

We finally stress that the findings of this section are specific to the EFT-extended Zee-Babu scenario. As we do not specify a concrete UV completion, the nature of the EFT insertions could be tree level- or loop-induced. This should be contrasted with other scalar extensions of the SM that contain charged states, e.g., the two Higgs doublet model which can address the anomalous magnetic moment of the muon (see, e.g., the recent [56]) beyond the one-loop approximation [57,58] in a fully renormalizable way.

B. Loop-induced $M_H = 125$ GeV Higgs physics

We now turn to the discussion of the impact of the model discussed in Sec. II on the loop-induced phenomenology of the 125 GeV Higgs boson. Assuming the narrow width approximation (NWA), we consider the signal strengths from dominant gluon fusion production [59] (see also [60–62]),

$$\mu_{gg}^X = \frac{[\sigma_{\text{GF}} \times \text{BR}(H \rightarrow X)]^{\text{BSM}}}{[\sigma_{\text{GF}} \times \text{BR}(H \rightarrow X)]^{\text{SM}}}. \quad (16)$$

The CMS experiment predicts [63] a sensitivity in the experimentally clean $H \rightarrow \gamma\gamma$ channel of

$$\frac{\Delta\mu_{gg}^{\gamma\gamma}}{\mu_{gg}^{\gamma\gamma}} = 3.3\%, \quad (17)$$

at a (HL-)LHC luminosity of 3/ab. Sensitivity in the $Z\gamma$ channel has been considered in [64] (for a recent analysis, see [65]) providing a HL-LHC estimate of

$$\frac{\Delta\mu_{gg}^{Z\gamma}}{\mu_{gg}^{Z\gamma}} = 18\%. \quad (18)$$

Mapping these sensitivity intervals onto BSM-modified SM predictions, we include the effective interactions of Sec. II to $H \rightarrow gg$ (which relates to Higgs production via unitarity [66]) and $H \rightarrow Z\gamma$, as well as $H \rightarrow \gamma\gamma$. This leads to one-loop sensitivity to the operators listed in Table III, including $\mathcal{O}_{\phi\mathcal{R}D}$ and $\mathcal{O}_{\phi\mathcal{S}D}$. Similar to our discussion in Sec. III A, the inclusion of BSMEFT interactions leads to a renormalization of the SMEFT counterparts as outlined in Ref. [67]. Here, we emphasize on the fact that the SM predictions for Higgs signal strengths in any other decay channels do not receive any modification from the charged scalar effective interactions.

TABLE III. The parameters and the singly and doubly charged scalar related operators which contribute to the corrections in prominent loop-induced H -decay modes.

Decay mode	Renormalisable couplings	Contributing operators
$H \rightarrow \gamma\gamma$	λ_4, λ_5	$\mathcal{O}_{\phi\mathcal{R}D}, \mathcal{O}_{\phi\mathcal{R}}, \mathcal{O}_{\phi\mathcal{S}},$ $\mathcal{O}_{\phi\mathcal{S}D}, \mathcal{O}_{B\mathcal{R}}, \mathcal{O}_{\bar{B}\mathcal{R}},$ $\mathcal{O}_{W\mathcal{R}}, \mathcal{O}_{\bar{W}\mathcal{R}}, \mathcal{O}_{B\mathcal{S}},$ $\mathcal{O}_{\bar{B}\mathcal{S}}, \mathcal{O}_{W\mathcal{S}}, \mathcal{O}_{\bar{W}\mathcal{S}}.$
$H \rightarrow Z\gamma$	λ_4, λ_5	$\mathcal{O}_{\phi\mathcal{R}D}, \mathcal{O}_{\mathcal{R}\phi D}, \mathcal{O}_{\phi\mathcal{R}},$ $\mathcal{O}_{\phi\mathcal{S}}, \mathcal{O}_{\phi\mathcal{S}D}, \mathcal{O}_{S\phi D},$ $\mathcal{O}_{B\mathcal{R}}, \mathcal{O}_{\bar{B}\mathcal{R}}, \mathcal{O}_{W\mathcal{R}},$ $\mathcal{O}_{\bar{W}\mathcal{R}}, \mathcal{O}_{B\mathcal{S}}, \mathcal{O}_{\bar{B}\mathcal{S}},$ $\mathcal{O}_{W\mathcal{S}}, \mathcal{O}_{\bar{W}\mathcal{S}}.$
$H \rightarrow gg$	λ_4, λ_5	$\mathcal{O}_{G\mathcal{R}}, \mathcal{O}_{\bar{G}\mathcal{R}},$ $\mathcal{O}_{G\mathcal{S}}, \mathcal{O}_{\bar{G}\mathcal{S}}.$

In Fig. 3, we demonstrate the impact of the renormalizable Zee-Babu scenario as well as the charged scalar effective interactions on the considered Higgs signal strength measurements. The BSM charged scalar interactions of the Zee-Babu Lagrangian modify both $H \rightarrow \gamma\gamma, Z\gamma$ branchings, especially in a lower mass range for the charged scalars, and the effect can be captured through λ_4 and λ_5 , as depicted by the solid lines in Fig. 3. The inclusion of the effective operator interactions, mentioned in Table III, can further lead to significant modifications of the branchings. We compare the effect from the dominantly contributing Wilson coefficients for h^\pm interactions $\mathcal{C}_{W\mathcal{S}}, \mathcal{C}_{B\mathcal{S}}$, and $r^{\pm\pm}$ related interactions $\mathcal{C}_{W\mathcal{R}}, \mathcal{C}_{B\mathcal{R}}$ on signal strength. We find from Figs. 3(a) and 3(c) that the doubly charged effective interactions dominate over the singly charged ones, but the dissimilarity vanishes as the new physics scale Λ moves away from the considered charged mass range, as can be seen in Figs. 3(b) and 3(d).

C. Direct LHC sensitivity to doubly charged scalars

The scalars of Sec. II can be produced at colliders via their hypercharge quantum numbers, implying a predominant production in pairs via Drell-Yan-like processes, which is common to many charged scalar extensions of the SM (see, e.g., [68–70]). The production of two $r^{\pm\pm}$ is more efficient than pair production of h^\pm due to its larger charge when assuming similar masses. It will also dominate over $r^{\pm\pm}r^*$ along with $r^* \rightarrow h^\mp h^\mp$ though a virtual r^* , see Ref. [39]. The $r^{\pm\pm}$ decay phenomenology that we consider in more detail in this section is characterized by decays $r^{\pm\pm} \rightarrow h^\pm h^\pm$ (when kinematically accessible),

$$\begin{aligned} \Gamma(r^{\pm\pm} \rightarrow h^\pm h^\pm) &= \frac{\beta}{128\pi M_{r^{\pm\pm}}} \left\{ 2\frac{\mathcal{C}_r}{\Lambda} v^2 + m \left(\frac{\mathcal{C}_{\phi\mathcal{R}D}}{\Lambda^2} v^2 + 2\frac{\mathcal{C}_{\phi\mathcal{S}D}}{\Lambda^2} v^2 - 4 \right) \right\}^2, \end{aligned} \quad (19)$$

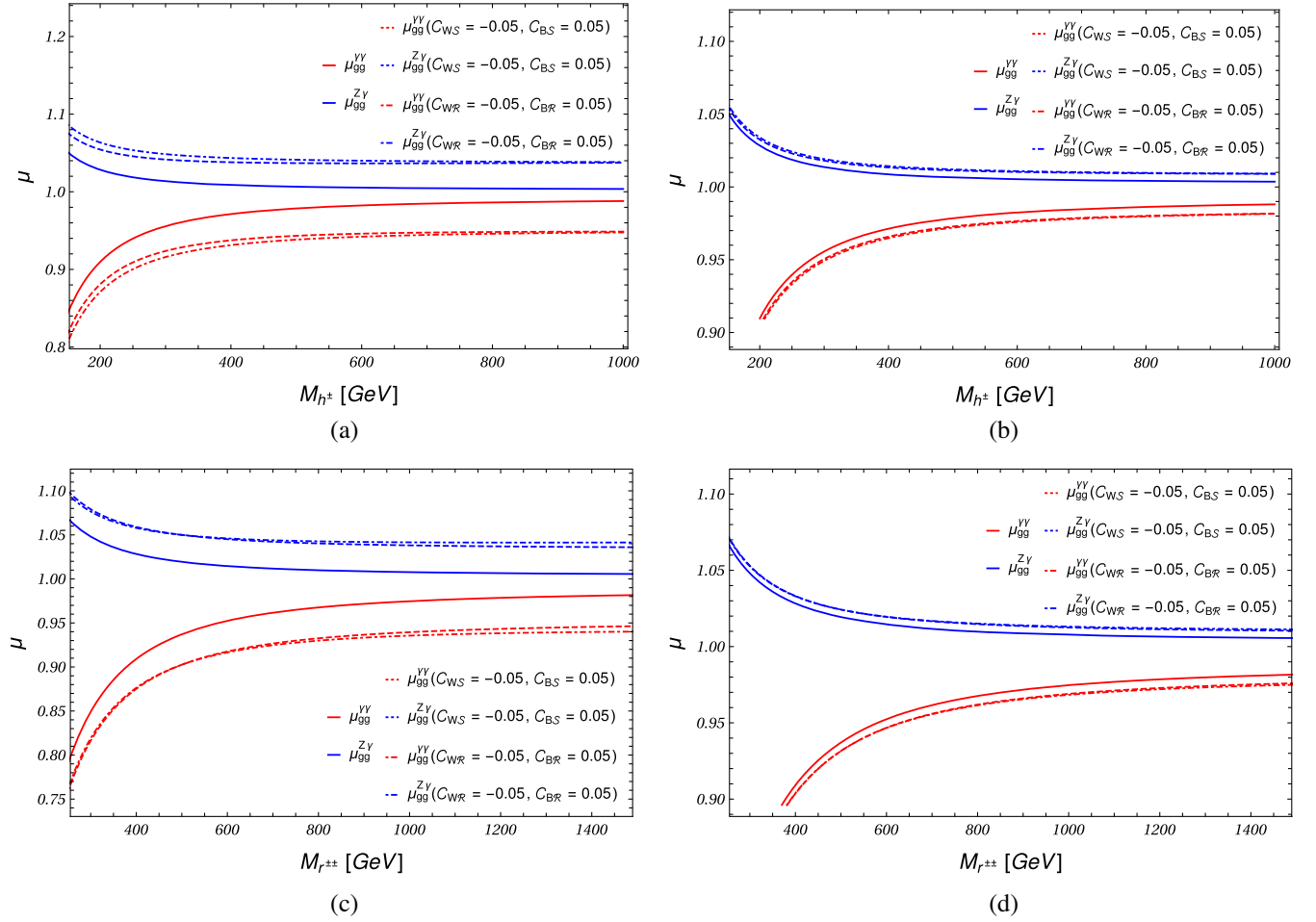


FIG. 3. Impact of the BSM parameters and representative effective operators on signal strength as a function of the charged scalar masses. The solid lines denote the effect of the Zee-Babu parameters λ_4 and λ_5 , whereas the dotted and the dotted-dashed lines show the impact of the h^\pm related C_{WS} , C_{BS} , and $r^{\pm\pm}$ related C_{WR} , C_{BR} , respectively. We consider $M_{r^{\pm\pm}} = 1.2$ TeV for (a) and (b) and $M_{h^\pm} = 0.5$ TeV for (c) and (d). We also show that for $\Lambda = 2$ TeV, the $r^{\pm\pm}$ interactions dominate over h^\pm interactions in (a) and (c), and in (b) and (d) the deviation vanishes for $\Lambda = 5$ TeV. We set $\lambda_4 = \lambda_5 = 1$ for all four plots.

where β is the h^\pm velocity in the $r^{\pm\pm}$ rest frame, as well as same sign lepton decays, e.g.,

$$\begin{aligned} \Gamma(r^{\pm\pm} \rightarrow \mu^\pm \mu^\pm) &= \frac{M_{r^{\pm\pm}}}{128\pi} \left\{ \left(4f_{\mathcal{R},\mu\mu} - [2C_{e\mathcal{R}\phi} + f_{\mathcal{R},\mu\mu}C_{\phi\mathcal{R}D}] \frac{v^2}{\Lambda^2} \right)^2 \right. \\ &\quad \left. + 4 \frac{C_{l\phi\mathcal{R}}^2}{\Lambda^4} v^2 \right\}, \end{aligned} \quad (20)$$

in the limit $m_{e^+} \ll M_{r^{\pm\pm}}$.⁵

In the Zee-Babu model, pair production of the doubly charged scalar through Drell-Yan $pp \rightarrow Z/A \rightarrow r^{++}r^{--}$ is only affected by the values of SM couplings, and any change in production rate arises through BSMEFT operators. Focusing on the overlap of contributing operators

⁵This extends the results of, e.g., Ref. [45] to EFT interactions. These results can be straightforwardly linearized in $\sim 1/\Lambda^2$.

between Drell-Yan, Higgs decays, and anomalous muon magnetic moment, we note that only $\mathcal{O}_{\phi\mathcal{R}D}$ contributes in the $r^{\pm\pm}$ pair production through a rescaling of the r field. Considering the possible subsequent decays with leptonic final states, we anticipate that the experimental sensitivity of channels with decays to h^\pm will be significantly impacted by the presence of neutrinos that appear as missing energy. Additionally, any final state involving tau leptons will yield a decreased sensitivity due to the difficulty in tagging them in detectors compared to muons and electrons. In contrast, the four lepton channel $r^{++}r^{--} \rightarrow \ell^+\ell^+\ell^-\ell^-$ will provide a clear signature with a suppressed SM background when the fact that $r^{\pm\pm}$ is the only particle in the model decaying to same-charge leptons is exploited in the analysis.

We model the new physics interactions using FeynRules [71,72] and exporting them in the UFO [73] format that can be imported in MadGraph [74]. Events for the Zee-Babu and BSMEFT are generated with MadEvent [74–76] including

only the interference effects of $\mathcal{O}_{\phi\mathcal{R}D}$. We include all SM processes contributing to $pp \rightarrow \ell^+\ell^-\ell^+\ell^-$ as background with a generation-level cut vetoing events in the $M_Z \pm 3.5\Gamma_Z$ interval, where M_Z and Γ_Z are the invariant mass and decay width of the (virtual) Z boson, respectively. Total decay widths for the charged scalars are calculated with MadWidth [77] and cross checked against our analytical results. The events are generated with a fixed branching ratio $\text{BR}(r^{\pm\pm} \rightarrow \ell^{\pm}\ell^{\pm})$, and we subsequently rescale the rates under the assumption of the NWA.

Our analysis is based on the ATLAS search for doubly charged scalars in Ref. [78] with relaxed cuts and is performed at a parton level to obtain a qualitative, proof-of-principle comparison. Selection of our analysis requires that all light leptons are in the central part of the detector ($|\eta(\ell)| < 2.5$) with a transverse momentum of $p_T(\ell) > 30$ GeV. Only leptons with no jet activity within the cone radius $\Delta R(j, \ell) = \sqrt{\Delta\eta^2 + \Delta\phi^2} < 0.4$ are considered, and we require exactly four leptons with one positively charged pair and one negatively charged; otherwise, the event is vetoed (we do not include charge mistagging or other experimental systematic uncertainties). A cut is imposed on the invariant mass of each pair such that $m_{\ell^{\pm}\ell^{\pm}} > 200$ GeV always. Since the same-charged leptons must be a result of $r^{\pm\pm}$ decays, we check the consistency of the two masses by calculating

$$\bar{M} = \frac{m_{\ell^+\ell^+} + m_{\ell^-\ell^-}}{2}, \quad (21)$$

and

$$\Delta M = |m_{\ell^+\ell^+} - m_{\ell^-\ell^-}|. \quad (22)$$

The two invariant masses are considered consistent if $\Delta M/\bar{M} < 0.25$ is satisfied, thus imposing the resonant signal character. Finally, the event is vetoed if a same-flavor, oppositely charged pair exists with invariant mass in the interval $m_{\ell^+\ell^-} \in [81.2, 101.2]$ GeV in order to suppress any background resulting from decays of Z bosons.

We evaluate the sensitivity of LHC using events measure from the \bar{M} differential distribution. Including the new physics contributions, the distribution is given by

$$\frac{d\sigma}{d\bar{M}} = \frac{d\sigma_{\text{SM}}}{d\bar{M}} + \frac{d\sigma_{\text{BZ}}}{d\bar{M}} + \frac{\mathcal{C}_{\phi\mathcal{R}D}}{\Lambda^2} \frac{d\sigma_{\phi\mathcal{R}D}}{d\bar{M}}, \quad (23)$$

where σ_{SM} denotes the Standard Model contribution and $\sigma_{\text{BZ}} = \sigma_{\text{BZ}}(f_{\mathcal{R}}, M_{r^{\pm\pm}}, M_{h^{\pm}})$ the pure Zee-Babu, which depends on the $f_{\mathcal{R}}$ coupling and the masses of $r^{\pm\pm}$ and h^{\pm} . The dimension-6 interference contribution from $\mathcal{O}_{\phi\mathcal{R}D}$ is denoted as $\sigma_{\phi\mathcal{R}D}$ and also depends on the same parameters as σ_{BZ} . The new physics contributions are rescaled with a K-factor value of 1.3 (see, e.g., [79]) to include higher order corrections. We note that the dependence on $f_{\mathcal{R}}$ and $M_{h^{\pm}}$

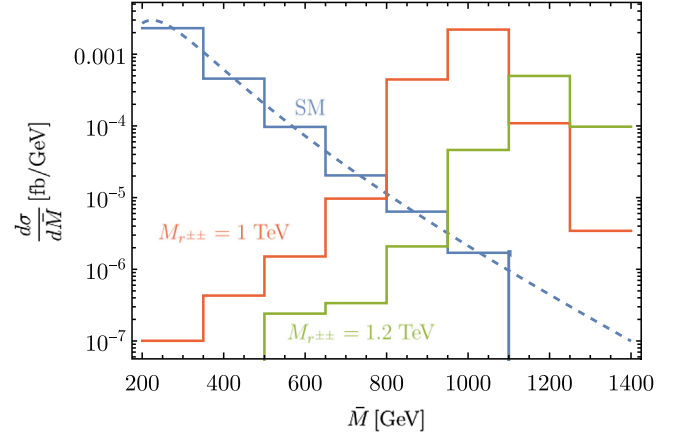


FIG. 4. \bar{M} distributions for the SM and new physics contributions. The dashed line shows the fit of the background and for the signal $f_{\mathcal{R}} = 0.1$, and a representative $\bar{\mathcal{C}}_{\phi\mathcal{R}D} = 0.3$ was used with the remaining BSMEFT WCs set to zero. The mass of the singly charged scalar is set to 480 (500) GeV for the scenario with $M_{r^{\pm\pm}} = 1$ TeV ($M_{r^{\pm\pm}} = 1.2$ TeV).

enters through the branching ratio $\text{BR}(r^{\pm\pm} \rightarrow \ell^{\pm}\ell^{\pm})$, and the ratio's dependence on $\mathcal{C}_{\phi\mathcal{R}D}$ cancels out when no other BSMEFT operator is included. This allows us to obtain contributions for different values of $f_{\mathcal{R}}$ by rescaling assuming the NWA and to generate events for interference effects caused by $\mathcal{O}_{\phi\mathcal{R}D}$ independent of $\mathcal{C}_{\phi\mathcal{R}D}$.

The \bar{M} distribution obtained from SM processes is fitted away from the signal region to obtain an experimentally driven estimate for the background for large values of \bar{M} . The \bar{M} distribution for particular values of new physics parameters is shown in Fig. 4. We evaluate the signal and background number of events in the region $\bar{M} > 200$ GeV at an integrated luminosity of $3/\text{ab}$ as S and B , respectively, and calculate the significance S/\sqrt{B} ($S/\sqrt{S+B}$) under the SM (new physics) hypothesis. We comment on the search's sensitivity in the next section.

IV. BSMEFT INTERPLAY

We are now ready to consider the phenomenological interplay of the observables discussed in the previous Sec. III.⁶ In Fig. 5, the Venn diagram shows the common operators contributing to all three processes discussed in Sec. III. A number of these operators contribute in a fermion mass-suppressed way. The dominant overlap of Higgs data, a_{μ} , and Drell-Yan production is therefore a single operator $\sim \mathcal{C}_{\phi\mathcal{R}D}$, which only affects the total width of the exotic scalar search. It is worthwhile to stress that when

⁶As indicated by the renormalization procedure, the measurements considered in this work would be part of the input data in a comprehensive global fit. In this work, we limit ourselves to the phenomenological interplay of the three measurement methodologies assuming vanishing SMEFT contributions.

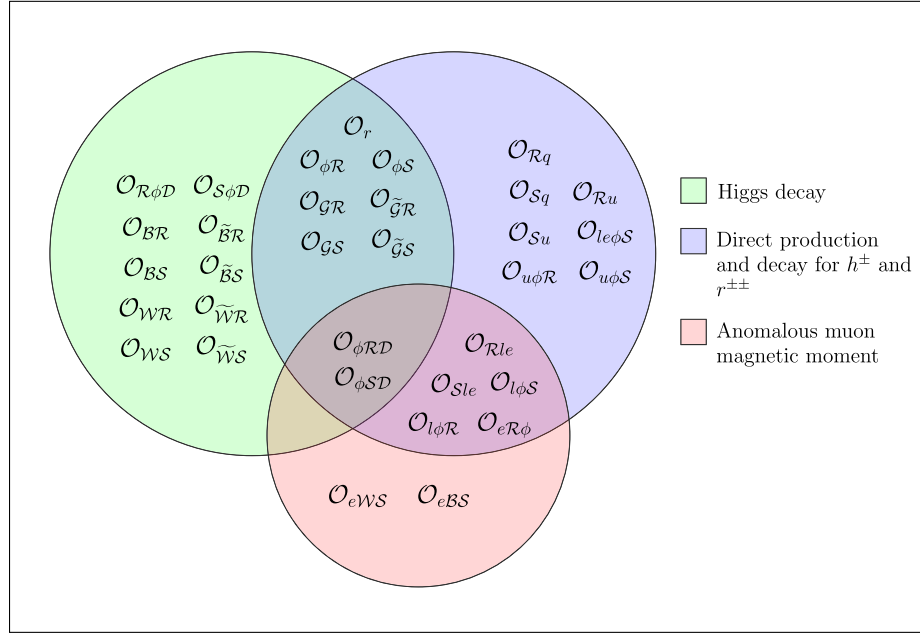


FIG. 5. Diagram depicting BSMEFT operators that contribute to three measurements considered in the calculation. $\mathcal{O}_r, \mathcal{O}_{\phi R}, \mathcal{O}_{\phi S}, \mathcal{O}_{GR}, \mathcal{O}_{\tilde{G}R}, \mathcal{O}_{GS}, \mathcal{O}_{\tilde{G}S}$ are the common operators contributing to both Higgs decay and processes relevant for direct detection for production and decay for charged scalars. $\mathcal{O}_{Rle}, \mathcal{O}_{Sle}, \mathcal{O}_{l\phi S}, \mathcal{O}_{l\phi R}, \mathcal{O}_{eR\phi}$ contribute to anomalous muon magnetic moment as well as charged scalar production and decay processes. $\mathcal{O}_{\phi RD}, \mathcal{O}_{\phi SD}$ contribute to all three processes. A range of the operators are mass suppressed thus leading to a small overlap in the limit of vanishing quark/lepton masses (e.g., when considering the parton model of LHC collisions).

we do not consider effective interactions related to h^\pm , the anomalous magnetic moment is predictive at $\mathcal{O}(\Lambda^{-2})$; i.e., the $r^{\pm\pm}$ contribution to Δa is finite even when EFT insertions are considered [see Eq. (15)]. The interplay of Higgs data, direct sensitivity in LHC searches, and anomalous magnetic moment is therefore relatively transparent in the scenario of Sec. II.

In Fig. 6, we show the interplay of the direct search outlined in Sec. III C with the anomalous magnetic moment for a particular mass choice of the exotic charged scalars (including open decays $r^{\pm\pm} \rightarrow h^\pm h^\pm$). The blue contour refers to the Fermilab a_μ measurement, while the red contour shows the SM expectation as provided in Ref. [23],

$$a_\mu(\text{SM}) = (116591810 \pm 43) \times 10^{-11}, \quad (24)$$

when the uncertainty is used as a limit for new physics. The size of the Fermilab/BNL excess can be compensated by contributions that can be attributed to new BSM physics, overcoming the limitations of the renormalizable Zee-Babu model; however, at strong coupling, $\mathcal{C}_{\phi RD} \text{ TeV}^2/\Lambda^2 \simeq 66$. This is due to the fact that the EFT contribution, while not being logarithmically enhanced, has to overcome the renormalizable contribution of the charged scalars. As already alluded to in Sec. III A, this can be mitigated by considering charged scalar contributions. Our $r^{\pm\pm}$ -related

findings are qualitatively similar to results reported in other model-specific a_μ analyses [25–33]; BSM states are forced to be light and/or strongly coupled to address the a_μ anomaly. Including signal extrapolations at the LHC as shown in Fig. 6(a) shows that any evidence for new doubly charged states at the LHC would stand in stark contrast with the a_μ measurement when interpreted from an extended Zee-Babu perspective.

Including Higgs physics (which is dominated by $\mu_{gg}^{\gamma\gamma}$) leads to further tension. Even when direct renormalizable trilinear $H - r^{++} - r^{--}$ couplings are dialed small $\lambda_5 \simeq 0$ [note that Eq. (8) includes this limit], $\mathcal{O}_{\phi RD}$ (see Table I) introduces the $r^{\pm\pm}$ loop contributions to the Higgs signal strength $\mu_{gg}^{\gamma\gamma}$, which at this point in the LHC program is already constrained at the 10% level. Scanning the Higgs signal strength modifications, including the h^\pm interactions and their dimension-6 EFT modifications, we are not able to reconcile SM consistency of the $H \rightarrow \gamma\gamma$ branching with the a_μ anomaly when the latter is attributed to choices in the $f_{\mathcal{R}} - \mathcal{C}_{\phi RD}$ plane.

Opening up the EFT and renormalizable coupling space, cancellations between the charged states and their EFT interactions can appear. This typically requires the full renormalization of a_μ as described above. For

$$\mathcal{C}_{\phi SD} = -4\mathcal{C}_{\phi RD}, \quad M_{r^{\pm\pm}} \simeq M_{S^\pm}, \quad (25)$$

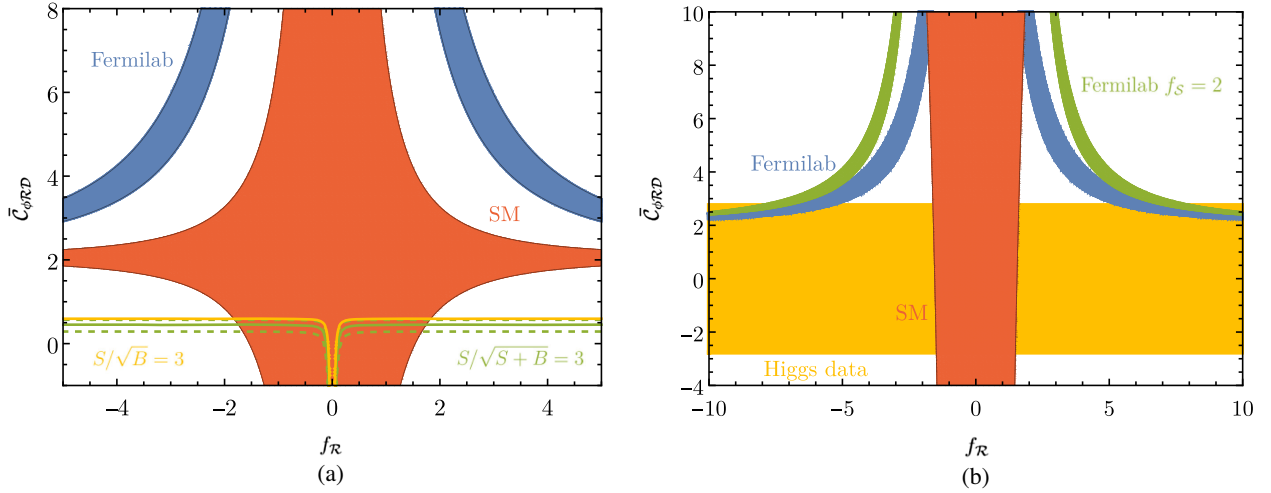


FIG. 6. Regions in the $f_{\mathcal{R}}-\bar{C}_{\phi\mathcal{R}D}$ plane, where $\bar{C}_i = C_i v^2/\Lambda^2$. Blue shows the parameter region where a_μ is in agreement with the Fermilab experimental measurement given in Eq. (2), while for points in the red region a_μ lies in the SM expectation range of Eq. (24). Both contours depend on f_S which has been set to zero, although we note that any value smaller than unity does not significantly affect the results. In the left panel, we set $M_{r^{\pm\pm}} = 1$ TeV and $M_{h^\pm} = 0.48$ TeV and also show the $S/\sqrt{B} = 3$ ($S/\sqrt{S+B} = 3$) contour for the direct detection analysis with yellow (green) using a value of $m = 246$ GeV. Note that strong EFT coupling (BSMEFT > BSM) is $|\bar{C}_{\phi\mathcal{R}D}| \gtrsim 0.8$. In the right panel, we restrict $\bar{C}_{\phi\mathcal{S}D} \approx -4\bar{C}_{\phi\mathcal{R}D}$ and set $M_{r^{\pm\pm}} = M_{h^\pm} = 1$ TeV. Additionally, we show the contours that yield agreement with the Fermilab measurement when $f_S = 2$ with green and overlay the results for the Higgs decay sensitivity from Eq. (17) for the choice of Eq. (25).

the charged Higgs contributions cancel. The a_μ excess could then be reproduced from a mismatch of the Yukawa couplings, see Fig. 6(b). We find that $f_{\mathcal{R}} \sim 5$ and $f_S \sim 1$ can accommodate the Fermilab excess for strong coupling $\bar{C}_{\phi\mathcal{R}D} \sim 3$, which implies a $r^{\pm\pm}$ partial width into a single lepton combination of around 60 GeV. Such a state can fall into the LHC kinematic coverage, see Fig. 6(a) and Ref. [78]. The further exploration of the high mass doubly charged scalar production is therefore highly motivated in the light of a SM-like Higgs and the consolidated a_μ anomaly.

V. CONCLUSIONS

The recent Fermilab consolidation of a_μ raises the question of how new physics can be accommodated as the exotics and Higgs precision program is evolving at the LHC. The direct sensitivity at the LHC with its so far null results in BSM searches moves new physics scales into regions where it becomes challenging to accommodate a significant anomalous magnetic moment of the muon when we take the BNL/Fermilab results as indication for BSM interactions. In this work, we have approached the interplay of these experimental arenas by means of EFT. A significant muon magnetic moment typically requires the presence of relatively light degrees of freedom (for a review of different scenarios see the recent Ref. [26]). In this work, we focus on light charged degrees of freedom, which we supplement with complete dimension-5 and -6 EFT

analyses to account for new dynamics that modify correlations away from patterns of renormalizable interactions. The Zee-Babu scenario as a particularly motivated BSM candidate theory gives then rise to a range of BSMEFT interactions that enable us to discuss a_μ precision results in tension with expected developments at the LHC.

Obviously, the rather large number of relevant Wilson coefficients exceeds the number of measurements that result from Higgs physics, a_μ , and direct sensitivity via $r^{\pm\pm}$ pair production, yet the overlapping set of operators that simultaneously affects all measurements and searches is relatively small and shows a significant tension when the SM expectation for Higgs physics is considered. Agreement of a_μ requires a significant deformation of charged scalar interactions, which in turn highly modify Higgs physics beyond experimentally allowed constraints. While this is particularly pronounced when we limit ourselves to the $r^{\pm\pm}$ state, we find that the additional freedom provided by the EFT extension of the h^\pm interactions can be exploited to achieve cancellations that render Higgs data compatible with the SM observation while obtaining a sizeable a_μ , again at relatively large couplings. On the one hand, this provides an important constraint for potential UV completions that the considered scenarios seeks to inform. On the other hand, the associated parameter ranges can be explored by future searches for doubly charged scalar states as done in, e.g., [65]. These very limiting conclusions only hold when we interpret the three different channels by focusing on the single overlapping

operator. As can be seen from Fig. 5, such a tension can be relieved by considering operators that do not contribute to all channels simultaneously. In such a case, additional channels need to be exploited to clarify a size of the muon anomalous coupling. Additional constraints can, in principle, be resolved in more challenging $pp \rightarrow 2\ell/4\ell + E_T$ searches, the impact of which we leave for future work.

ACKNOWLEDGMENTS

The work of Anisha, U. B., and J. C. is supported by the Science and Engineering Research Board, Government of India, under the agreement SERB/PHY/2019501 (MATRICS). C. E. is supported by the UK Science and Technology Facilities Council (STFC) under Grant No. ST/T000945/1 and by the IPPP Associateship Scheme. M. S. is supported by the STFC under Grant No. ST/P001246/1. P. S. is funded by an STFC studentship under Grant No. ST/T506102/1.

APPENDIX A: BSM EFFECTIVE OPERATORS

Throughout the paper, we assume that the charged scalars \mathcal{S} and \mathcal{R} are light enough to be considered as infrared degrees of freedom. Thus, after integrating out the new physics at Λ , we are left with effective operators that lead to the modifications of SM interactions (i.e., the SMEFT operators) or can alter the existent BSM interactions at the renormalizable level and are hereby identified as BSMEFT operators.

The general way to capture the effect of all possible such modifications is to construct a complete and exhaustive set of BSMEFT operators at each mass dimension following a bottom-up approach. A number of models where SM is extended by new degrees of freedom have been discussed in Ref. [80].

We generated Warsaw-like operator bases of dimension-5 and -6 operators for the case of the Zee-Babu model with GrIP [81]; the explicit structures of these operators have been tabulated in Tables IV, V, and VI. Notably, we obtain a new class of dimension-5 operators Φ^5 , which unlike for the SMEFT case, arise due to possible gauge invariant

TABLE IV. Explicit structures of the dimension-5 effective operators for the Zee-Babu model. The operators written in bold have distinct Hermitian conjugates.

Φ^5			
\mathcal{O}_r	$(\phi^\dagger \phi) \mathcal{R}^\dagger \mathcal{S}^2$	\mathcal{O}_{sr}	$(\mathcal{S}^\dagger \mathcal{S}) \mathcal{R}^\dagger \mathcal{S}^2$
\mathcal{O}_{rs}	$(\mathcal{R}^\dagger \mathcal{R}) \mathcal{R}^\dagger \mathcal{S}^2$		
$\Psi^2 \Phi^2$			
$\tilde{\mathcal{O}}_{dq\phi\mathcal{S}}$	$(\tilde{Q}d)(\tilde{\phi}\mathcal{S})$	$\tilde{\mathcal{O}}_{uq\phi\mathcal{S}}$	$(\tilde{Q}u)(\phi\mathcal{S})$
$\tilde{\mathcal{O}}_{le\phi\mathcal{S}}$	$(\tilde{L}e)(\tilde{\phi}\mathcal{S})$	$\tilde{\mathcal{O}}_{e\mathcal{S}}$	$(\bar{e}^c e) \mathcal{S}^2$

TABLE V. Explicit structures of the dimension-6 effective operators for the Zee-Babu model. The operators written in bold have distinct Hermitian conjugates.

Φ^6		$\Phi^4 \mathcal{D}^2$	
\mathcal{O}_S	$(\mathcal{S}^\dagger \mathcal{S})^3$	$\mathcal{O}_{S\Box}$	$(\mathcal{S}^\dagger \mathcal{S}) \Box (\mathcal{S}^\dagger \mathcal{S})$
$\mathcal{O}_{S\phi}$	$(\phi^\dagger \phi) (\mathcal{S}^\dagger \mathcal{S})^2$	$\mathcal{O}_{S\phi\mathcal{D}}$	$(\mathcal{S}^\dagger \mathcal{S}) [(\mathcal{D}^\mu \phi)^\dagger (\mathcal{D}_\mu \phi)]$
$\mathcal{O}_{\phi\mathcal{S}}$	$(\phi^\dagger \phi)^2 (\mathcal{S}^\dagger \mathcal{S})$	$\mathcal{O}_{\phi\mathcal{S}\mathcal{D}}$	$(\phi^\dagger \phi) [(\mathcal{D}^\mu \mathcal{S})^\dagger (\mathcal{D}_\mu \mathcal{S})]$
$\mathcal{O}_{\mathcal{R}}$	$(\mathcal{R}^\dagger \mathcal{R})^3$	$\mathcal{O}_{\mathcal{R}\Box}$	$(\mathcal{R}^\dagger \mathcal{R}) \Box (\mathcal{R}^\dagger \mathcal{R})$
$\mathcal{O}_{\mathcal{R}\phi}$	$(\phi^\dagger \phi) (\mathcal{R}^\dagger \mathcal{R})^2$	$\mathcal{O}_{\mathcal{R}\phi\mathcal{D}}$	$(\mathcal{R}^\dagger \mathcal{R}) [(\mathcal{D}^\mu \phi)^\dagger (\mathcal{D}_\mu \phi)]$
$\mathcal{O}_{\phi\mathcal{R}}$	$(\phi^\dagger \phi)^2 (\mathcal{R}^\dagger \mathcal{R})$	$\mathcal{O}_{\phi\mathcal{R}\mathcal{D}}$	$(\phi^\dagger \phi) [(\mathcal{D}^\mu \mathcal{R})^\dagger (\mathcal{D}_\mu \mathcal{R})]$
$\mathcal{O}_{\phi\mathcal{R}\mathcal{S}}$	$(\phi^\dagger \phi) (\mathcal{R}^\dagger \mathcal{R}) (\mathcal{S}^\dagger \mathcal{S})$	$\mathcal{O}_{S\mathcal{R}\mathcal{D}}$	$(\mathcal{S}^\dagger \mathcal{S}) [(\mathcal{D}^\mu \mathcal{R})^\dagger (\mathcal{D}_\mu \mathcal{R})]$
$\mathcal{O}_{S\mathcal{R}}$	$(\mathcal{S}^\dagger \mathcal{S})^2 (\mathcal{R}^\dagger \mathcal{R})$	$\mathcal{O}_{\mathcal{R}\mathcal{S}\mathcal{D}}$	$(\mathcal{R}^\dagger \mathcal{R}) [(\mathcal{D}^\mu \mathcal{S})^\dagger (\mathcal{D}_\mu \mathcal{S})]$
$\mathcal{O}_{\mathcal{R}\mathcal{S}}$	$(\mathcal{S}^\dagger \mathcal{S}) (\mathcal{R}^\dagger \mathcal{R})^2$	$\mathcal{O}_{\phi\mathcal{S}\mathcal{R}\mathcal{D}}$	$(\mathcal{S}^\dagger \mathcal{R}) [(\mathcal{D}^\mu \tilde{\phi}^\dagger) (\mathcal{D}_\mu \tilde{\phi})]$
$\mathcal{O}_{S^2\mathcal{R}}$	$(\mathcal{S}\mathcal{R}^\dagger \mathcal{S})^2$		
$\Phi^2 \chi^2$		$\Psi^2 \Phi^2 \mathcal{D}$	
\mathcal{O}_{BS}	$B_{\mu\nu} B^{\mu\nu} (\mathcal{S}^\dagger \mathcal{S})$	\mathcal{O}_{Sq}	$(\bar{Q}\gamma^\mu Q) (\mathcal{S}^\dagger i\overleftrightarrow{\mathcal{D}}_\mu \mathcal{S})$
\mathcal{O}_{BR}	$B_{\mu\nu} B^{\mu\nu} (\mathcal{R}^\dagger \mathcal{R})$	\mathcal{O}_{Rq}	$(\bar{Q}\gamma^\mu Q) (\mathcal{R}^\dagger i\overleftrightarrow{\mathcal{D}}_\mu \mathcal{R})$
$\mathcal{O}_{\tilde{B}S}$	$\tilde{B}_{\mu\nu} B^{\mu\nu} (\mathcal{S}^\dagger \mathcal{S})$	\mathcal{O}_{Sl}	$(\bar{L}\gamma^\mu L) (\mathcal{S}^\dagger i\overleftrightarrow{\mathcal{D}}_\mu \mathcal{S})$
$\mathcal{O}_{\tilde{B}R}$	$\tilde{B}_{\mu\nu} B^{\mu\nu} (\mathcal{R}^\dagger \mathcal{R})$	\mathcal{O}_{Rl}	$(\bar{L}\gamma^\mu L) (\mathcal{R}^\dagger i\overleftrightarrow{\mathcal{D}}_\mu \mathcal{R})$
\mathcal{O}_{GS}	$G_{\mu\nu}^A G^{A\mu\nu} (\mathcal{S}^\dagger \mathcal{S})$	\mathcal{O}_{Su}	$(\bar{u}\gamma^\mu u) (\mathcal{S}^\dagger i\overleftrightarrow{\mathcal{D}}_\mu \mathcal{S})$
\mathcal{O}_{GR}	$G_{\mu\nu}^A G^{A\mu\nu} (\mathcal{R}^\dagger \mathcal{R})$	\mathcal{O}_{Ru}	$(\bar{u}\gamma^\mu u) (\mathcal{R}^\dagger i\overleftrightarrow{\mathcal{D}}_\mu \mathcal{R})$
$\mathcal{O}_{\tilde{G}S}$	$\tilde{G}_{\mu\nu}^A G^{A\mu\nu} (\mathcal{S}^\dagger \mathcal{S})$	\mathcal{O}_{Sd}	$(\bar{d}\gamma^\mu d) (\mathcal{S}^\dagger i\overleftrightarrow{\mathcal{D}}_\mu \mathcal{S})$
$\mathcal{O}_{\tilde{G}R}$	$\tilde{G}_{\mu\nu}^A G^{A\mu\nu} (\mathcal{R}^\dagger \mathcal{R})$	\mathcal{O}_{Rd}	$(\bar{d}\gamma^\mu d) (\mathcal{R}^\dagger i\overleftrightarrow{\mathcal{D}}_\mu \mathcal{R})$
\mathcal{O}_{WS}	$W_{\mu\nu}^I W^{I\mu\nu} (\mathcal{S}^\dagger \mathcal{S})$	\mathcal{O}_{Se}	$(\bar{e}\gamma^\mu e) (\mathcal{S}^\dagger i\overleftrightarrow{\mathcal{D}}_\mu \mathcal{S})$
\mathcal{O}_{WR}	$W_{\mu\nu}^I W^{I\mu\nu} (\mathcal{R}^\dagger \mathcal{R})$	\mathcal{O}_{Re}	$(\bar{e}\gamma^\mu e) (\mathcal{R}^\dagger i\overleftrightarrow{\mathcal{D}}_\mu \mathcal{R})$
$\mathcal{O}_{\tilde{W}S}$	$\tilde{W}_{\mu\nu}^I W^{I\mu\nu} (\mathcal{S}^\dagger \mathcal{S})$	\mathcal{O}_{Sle}	$(\bar{L}^c \gamma^\mu e) (\tilde{\phi} i\mathcal{D}_\mu \mathcal{S})$
$\mathcal{O}_{\tilde{W}R}$	$\tilde{W}_{\mu\nu}^I W^{I\mu\nu} (\mathcal{R}^\dagger \mathcal{R})$	\mathcal{O}_{Rle}	$(\bar{L}^c \gamma^\mu e) (\phi i\mathcal{D}_\mu \mathcal{R})$

TABLE VI. Explicit structures of the dimension-6 effective operators for the Zee-Babu model. The operators written in bold have distinct Hermitian conjugates.

$\Psi^2 \Phi^3$			
$\mathcal{O}_{e\phi\mathcal{S}}$	$(\bar{L}e)\phi (\mathcal{S}^\dagger \mathcal{S})$	$\mathcal{O}_{l\phi\mathcal{S}}$	$(\bar{L}^c i\tau_2 L) \mathcal{S} (\phi^\dagger \phi)$
$\mathcal{O}_{u\phi\mathcal{S}}$	$(\bar{Q}u)\tilde{\phi} (\mathcal{S}^\dagger \mathcal{S})$	$\mathcal{O}_{l\mathcal{S}}$	$(\bar{L}^c i\tau_2 L) \mathcal{S} (\mathcal{S}^\dagger \mathcal{S})$
$\mathcal{O}_{d\phi\mathcal{S}}$	$(\bar{Q}d)\phi (\mathcal{S}^\dagger \mathcal{S})$	$\mathcal{O}_{e\mathcal{R}\phi}$	$(\bar{e}^c e) \mathcal{R} (\phi^\dagger \phi)$
$\mathcal{O}_{e\phi\mathcal{R}}$	$(\bar{L}e)\phi (\mathcal{R}^\dagger \mathcal{R})$	$\mathcal{O}_{l\phi\mathcal{R}}$	$(\bar{L}^c i\tau_2 L) (\phi^\dagger \mathcal{R}\tilde{\phi})$
$\mathcal{O}_{u\phi\mathcal{R}}$	$(\bar{Q}u)\tilde{\phi} (\mathcal{R}^\dagger \mathcal{R})$	$\mathcal{O}_{e\mathcal{R}}$	$(\bar{e}^c e) \mathcal{R} (\mathcal{R}^\dagger \mathcal{R})$
$\mathcal{O}_{d\phi\mathcal{R}}$	$(\bar{Q}d)\phi (\mathcal{R}^\dagger \mathcal{R})$	$\mathcal{O}_{e\mathcal{S}\mathcal{R}}$	$(\bar{e}^c e) \mathcal{R} (\mathcal{S}^\dagger \mathcal{S})$
$\mathcal{O}_{d\phi\mathcal{R}\mathcal{S}}$	$(\bar{Q}d)\tilde{\phi} (\mathcal{S}^\dagger \mathcal{R})$	$\mathcal{O}_{u\phi\mathcal{R}\mathcal{S}}$	$(\bar{Q}u)\phi (\mathcal{R}^\dagger \mathcal{S})$
$\Psi^2 \Phi \chi$			
\mathcal{O}_{eBS}	$B_{\mu\nu} (\bar{L}^c \sigma^{\mu\nu} L) \mathcal{S}$	\mathcal{O}_{eWS}	$W_{\mu\nu}^I (\bar{L}^c \tau^I \sigma^{\mu\nu} L) \mathcal{S}$
\mathcal{O}_{eBR}	$B_{\mu\nu} (\bar{e}^c \sigma^{\mu\nu} e) \mathcal{R}$		

structures allowed by hypercharge quantum numbers of the charged scalars.

APPENDIX B: RENORMALIZATION

In the following section, we provide the expressions for the renormalization constants (RC) which we include in the counterterms considered to remove the divergences for the calculation of muon anomalous magnetic moment and Higgs decay to diphoton, as discussed in Secs. III A and III B, respectively. For both scenarios, we choose on-shell renormalization for propagating fields and parameters and $\overline{\text{MS}}$ renormalization for the Wilson coefficients. The notations used here to express the one-point and the two-point integrals are given along the lines of Ref. [67],

$$A_0(m^2) = m^2 \Delta + \mathcal{O}(1),$$

$$B_0 = \Delta + \mathcal{O}(1),$$

$$B_1 = -\frac{\Delta}{2} + \mathcal{O}(1),$$

$$B_{00}(p^2, m_1^2, m_2^2) = \left(\frac{m_1^2 + m_2^2}{4} - \frac{p^2}{12} \right) \Delta + \mathcal{O}(1),$$

where Δ denotes the UV-divergent parts associated with the loop integrals which we remove via the renormalization of the Wilson coefficients (see, e.g., [49,50]). The functions dB_i represent the derivative of the scalar functions B_i with respect to the external momentum. Throughout our work, we express the RCs up to the order of Λ^{-2} and consistently neglect higher order corrections.

1. a_μ computation

We evaluate a_μ from a one-loop $\mu \rightarrow \mu\gamma$ vertex function, which requires one to consider both δZ_{AA} and δZ_{ZA} wave function RCs due to the $Z - \gamma$ mixing. Their explicit expressions computed from on-shell conditions are given as

$$\begin{aligned} \delta Z_{AA} = & \left[\frac{g_Y^2 g_W^2}{24(g_Y^2 + g_W^2)\pi^2} + \frac{5g_Y^2 g_W^2 B_0(M_W^2)}{16(g_Y^2 + g_W^2)\pi^2} + \frac{g_Y^2 g_W^2 B_1(M_W^2)}{8(g_Y^2 + g_W^2)\pi^2} + \frac{g_Y^2 g_W^2 M_W^2 dB_0(M_W^2)}{8(g_Y^2 + g_W^2)\pi^2} - \frac{g_Y^2 g_W^4 v^2 dB_0(M_W^2)}{32(g_Y^2 + g_W^2)\pi^2} \right. \\ & + \frac{g_Y^2 g_W^2 dB_{00}(M_{r^{\pm\pm}}^2)}{(g_Y^2 + g_W^2)\pi^2} + \frac{g_Y^2 g_W^2 (dB_{00}(M_{h^\pm}^2) + 3dB_{00}(M_W^2))}{4(g_Y^2 + g_W^2)\pi^2} + \sum_{l=e,\mu,\tau} \frac{g_Y^2 g_W^2 B_1(M_l^2)}{4(g_Y^2 + g_W^2)\pi^2} + \sum_{q_u=u,c,t} \frac{g_Y^2 g_W^2 B_1(M_{q_u}^2)}{3(g_Y^2 + g_W^2)\pi^2} \\ & \left. + \sum_{q_d=d,s,b} \frac{g_Y^2 g_W^2 B_1(M_{q_d}^2)}{12(g_Y^2 + g_W^2)\pi^2} - \sum_{l=e,\mu,\tau} \frac{2g_Y^2 g_W^2 dB_{00}(M_l^2)}{2(g_Y^2 + g_W^2)\pi^2} - \sum_{q_u=u,c,t} \frac{2g_Y^2 g_W^2 dB_{00}(M_{q_u}^2)}{3(g_Y^2 + g_W^2)\pi^2} - \sum_{q_d=d,s,b} \frac{g_Y^2 g_W^2 dB_{00}(M_{q_d}^2)}{6(g_Y^2 + g_W^2)\pi^2} \right], \quad (\text{B1}) \end{aligned}$$

and

$$\begin{aligned} \delta Z_{AZ} = & \left[\frac{g_Y g_W^3}{12(g_Y^2 + g_W^2)\pi^2} + \frac{g_Y^3 g_W (4A_0(M_{r^{\pm\pm}}^2) + A_0(M_{h^\pm}^2))}{4(g_Y^2 + g_W^2)M_Z^2 \pi^2} - \sum_{l=e,\mu,\tau} \frac{g_Y g_W (3g_Y^2 A_0(M_l^2) + g_W^2 A_0(M_l^2))}{8(g_Y^2 + g_W^2)M_Z^2 \pi^2} \right. \\ & + \sum_{q_d=d,s,b} \frac{g_Y g_W (3g_W^2 A_0(M_{q_d}^2) - g_Y^2 A_0(M_{q_d}^2))}{24(g_Y^2 + g_W^2)M_Z^2 \pi^2} + \sum_{q_u=u,c,t} \frac{g_Y g_W (3g_W^2 A_0(M_{q_u}^2) - 5g_Y^2 A_0(M_{q_u}^2))}{12(g_Y^2 + g_W^2)M_Z^2 \pi^2} \\ & + \frac{g_Y g_W}{16(g_Y^2 + g_W^2)M_Z^2 \pi^2} B_{00}(M_Z^2, M_W^2) (10g_W^2 M_Z^2 + 4g_W^2 M_W^2 + g_Y^2 g_W^2 v^2 - 4g_Y^2 + 10g_W^2) \\ & + \frac{g_Y g_W (g_Y^2 A_0(M_W^2) - 5g_W^2 A_0(M_W^2))}{8(g_Y^2 + g_W^2)M_Z^2 \pi^2} + \frac{g_Y^3 g_W (B_{00}(M_Z^2, M_{h^\pm}^2) - 4B_{00}(M_Z^2, M_{r^{\pm\pm}}^2))}{2(g_Y^2 + g_W^2)M_Z^2 \pi^2} \\ & + \sum_{l=e,\mu,\tau} \frac{g_Y g_W (3g_Y^2 - g_W^2) B_{00}(M_Z^2, M_l^2)}{4(g_Y^2 + g_W^2)M_Z^2 \pi^2} + \sum_{q_d=d,s,b} \frac{g_Y g_W (g_Y^2 - 3g_W^2) B_{00}(M_Z^2, M_{q_d}^2)}{12(g_Y^2 + g_W^2)M_Z^2 \pi^2} \\ & + \sum_{q_u=u,c,t} \frac{g_Y g_W (5g_Y^2 - 3g_W^2) B_{00}(M_Z^2, M_{q_u}^2)}{6(g_Y^2 + g_W^2)M_Z^2 \pi^2} + \sum_{f=l,q_u,q_d} \frac{g_Y g_W (g_W^2 - 3g_Y^2) B_1(M_Z^2, M_f^2)}{8(g_Y^2 + g_W^2)M_Z^2 \pi^2} + \frac{g_Y g_W^3 B_1(M_Z^2, M_W^2)}{4(g_Y^2 + g_W^2)\pi^2} \\ & \left. + \frac{g_Y g_W}{2(g_Y^2 + g_W^2)\pi^2} \left[\left(\frac{C_{B\mathcal{R}} - C_{W\mathcal{R}}}{\Lambda^2} \right) A_0(M_{r^{\pm\pm}}^2) + \left(\frac{C_{BS} - C_{WS}}{\Lambda^2} \right) A_0(M_{h^\pm}^2) \right], \quad (\text{B2}) \end{aligned}$$

respectively.

Similarly, we include the wave function renormalization for the left and right chiral components of external muon fields,

$$\begin{aligned}
\delta Z_{f_L} = & \left[\frac{(g_Y^4 + 4g_Y^2 g_W^2 + 3g_W^4)}{64(g_Y^2 + g_W^2)\pi^2} - \frac{f_{\mathcal{R}}^2 M_\mu^2 (dB_0(M_\mu^2, M_{r^{\pm\pm}}^2) - dB_1(M_\mu^2, M_{r^{\pm\pm}}^2))}{4\pi^2} - \frac{f_{\mathcal{S}}^2 (B_0(M_\mu^2, M_{h^\pm}^2) - B_1(M_\mu^2, M_{h^\pm}^2))}{8\pi^2} \right. \\
& - \frac{f_{\mathcal{S}}^2 M_\mu^2 (dB_0(M_\mu^2, M_{h^\pm}^2) - dB_1(M_\mu^2, M_{h^\pm}^2))}{8\pi^2} - \frac{g_Y^2 g_W^2}{8(g_Y^2 + g_W^2)\pi^2} (B_0(M_\mu^2, M_\mu^2) - B_1(M_\mu^2, M_\mu^2) + 2M_\mu^2 (dB_0(M_\mu^2, M_\mu^2) \\
& - dB_1(M_\mu^2, M_\mu^2))) - \frac{g_W^2 (g_Y^2 + g_W^2) (B_0(M_\mu^2, M_W^2) + B_1(M_\mu^2, M_W^2))}{16(g_Y^2 + g_W^2)\pi^2} - \frac{(g_Y^2 - g_W^2)^2 (B_0(M_\mu^2, M_Z^2) + B_0(M_\mu^2, M_W^2))}{32(g_Y^2 + g_W^2)\pi^2} \\
& - \frac{M_\mu^2 (B_0(M_\mu^2, M_H^2) - B_1(M_\mu^2, M_H^2))}{16\pi^2 v^2} - \frac{M_\mu^2 (B_0(M_\mu^2, M_Z^2) - B_1(M_\mu^2, M_Z^2))}{16\pi^2 v^2} - \frac{M_\mu^4}{8\pi^2 v^2} (dB_0(M_\mu^2, M_W^2) \\
& + dB_1(M_\mu^2, M_W^2) - 2dB_0(M_\mu^2, M_H^2) + dB_1(M_\mu^2, M_H^2) - dB_1(M_\mu^2, M_Z^2)) \left. \right] + \frac{v^2 (2f_{\mathcal{R}}^2 \mathcal{C}_{\phi\mathcal{R}\mathcal{D}} + f_{\mathcal{S}}^2 \mathcal{C}_{\phi\mathcal{S}\mathcal{D}} + f_{\mathcal{S}} \mathcal{C}_{l\phi\mathcal{S}})}{16\pi^2 \Lambda^2} \\
& \times [(B_0(M_\mu^2, M_{r^{\pm\pm}}^2) + B_1(M_\mu^2, M_{r^{\pm\pm}}^2)) + M_\mu^2 (dB_0(M_\mu^2, M_{r^{\pm\pm}}^2) + dB_1(M_\mu^2, M_{r^{\pm\pm}}^2))] \\
& + \frac{M_\mu^2 v^2 f_{\mathcal{R}} \mathcal{C}_{e\mathcal{R}\phi}}{4\pi^2 \Lambda^2} [(dB_0(M_\mu^2, M_{r^{\pm\pm}}^2) + dB_1(M_\mu^2, M_{r^{\pm\pm}}^2))] + \frac{f_{\mathcal{R}} M_\mu^2 v^2 \mathcal{C}_{l\phi\mathcal{R}}}{4\pi^2 \Lambda^2} dB_0(M_\mu^2, M_{r^{\pm\pm}}^2) \\
& + \frac{f_{\mathcal{R}} M_\mu v \mathcal{C}_{\mathcal{R}le}}{4\sqrt{2}\pi^2 \Lambda^2} [B_0(M_\mu^2, M_{r^{\pm\pm}}^2) + B_1(M_\mu^2, M_{r^{\pm\pm}}^2) + 2M_\mu^2 dB_0(M_\mu^2, M_{r^{\pm\pm}}^2)] \\
& + \frac{f_{\mathcal{S}} M_\mu v \mathcal{C}_{\mathcal{S}le}}{4\sqrt{2}\pi^2 \Lambda^2} [B_0(M_\mu^2, M_{r^{\pm\pm}}^2) + B_1(M_\mu^2, M_{r^{\pm\pm}}^2) + 2M_\mu^2 (dB_0(M_\mu^2, M_{r^{\pm\pm}}^2) + dB_1(M_\mu^2, M_{r^{\pm\pm}}^2))], \tag{B3}
\end{aligned}$$

and

$$\begin{aligned}
\delta Z_{f_R} = & \left[\frac{g_Y^2}{16\pi^2} - \frac{g_Y^4 (B_0(M_Z^2, M_\mu^2) + B_1(M_Z^2, M_\mu^2))}{8(g_Y^2 + g_W^2)\pi^2} - \frac{f_{\mathcal{R}}^2}{4\pi^2} (B_0(M_{r^{\pm\pm}}^2, M_\mu^2) + B_1(M_{r^{\pm\pm}}^2, M_\mu^2)) \right. \\
& + M_\mu^2 (dB_0(M_{r^{\pm\pm}}^2, M_\mu^2), dB_1(M_{r^{\pm\pm}}^2, M_\mu^2)) - \frac{f_{\mathcal{S}}^2 M_\mu^2}{8\pi^2} (dB_0(M_{h^\pm}^2, M_\mu^2) + dB_1(M_{h^\pm}^2, M_\mu^2)) \\
& - \frac{g_Y^2 g_W^2}{8(g_Y^2 + g_W^2)\pi^2} (B_0(M_\mu^2, M_\mu^2) + B_1(M_\mu^2, M_\mu^2) - 2(dB_0(M_\mu^2, M_\mu^2) + dB_1(M_\mu^2, M_\mu^2))) \\
& - \frac{M_\mu^2}{16\pi^2 v^2} (2B_0(M_W^2, M_\mu^2) + B_0(M_{h^\pm}^2, M_\mu^2) + 2B_1(M_W^2, M_\mu^2) + B_0(M_Z^2, M_\mu^2) - B_1(M_Z^2, M_\mu^2)) \\
& - \frac{M_\mu^2}{32(g_Y^2 + g_W^2)\pi^2} (8g_Y^2 g_W^2 dB_0(M_\mu^2, M_\mu^2) + (3g_Y^4 - 3g_Y^2 g_W^2 - g_Y^4) dB_0(M_Z^2, M_\mu^2) - g_Y^2 g_W^2 dB_1(M_\mu^2, M_\mu^2) \\
& - (5g_Y^4 - 2g_Y^2 g_W^2 + g_W^4) dB_1(M_Z^2, M_\mu^2)) - \frac{M_\mu^4}{8\pi^2 v^2} (dB_0(M_W^2, M_\mu^2) + 2dB_0(M_{h^\pm}^2, M_\mu^2) + dB_1(M_{h^\pm}^2, M_\mu^2) \\
& + dB_1(M_W^2, M_\mu^2) + dB_1(M_Z^2, M_\mu^2)) \left. \right] + \frac{\mathcal{C}_{\phi\mathcal{R}\mathcal{D}} f_{\mathcal{R}}^2 v^2}{8\pi^2 \Lambda^2} [B_0(M_{h^\pm}^2, M_\mu^2) + B_1(M_{h^\pm}^2, M_\mu^2) \\
& + M_\mu^2 (dB_0(M_{h^\pm}^2, M_\mu^2) dB_1(M_{h^\pm}^2, M_\mu^2))] + \frac{\mathcal{C}_{\phi\mathcal{S}\mathcal{D}} f_{\mathcal{S}}^2 M_\mu^2 v^2}{16\pi^2 \Lambda^2} [dB_0(M_{h^\pm}^2, M_\mu^2) + dB_1(M_{h^\pm}^2, M_\mu^2)] \\
& + \frac{\mathcal{C}_{e\mathcal{R}\phi} f_{\mathcal{R}} v^2}{4\pi^2 \Lambda^2} [B_0(M_{r^{\pm\pm}}^2, M_\mu^2) + B_1(M_{r^{\pm\pm}}^2, M_\mu^2) + M_\mu^2 (dB_0(M_{r^{\pm\pm}}^2, M_\mu^2) + dB_1(M_{r^{\pm\pm}}^2, M_\mu^2))] \\
& + \frac{\mathcal{C}_{l\phi\mathcal{R}} f_{\mathcal{R}} M_\mu^2 v^2 dB_0(M_{r^{\pm\pm}}^2, M_\mu^2)}{4\pi^2 \Lambda^2} + \frac{\mathcal{C}_{l\phi\mathcal{S}} f_{\mathcal{S}} M_\mu^2 v^2}{16\pi^2 \Lambda^2} [dB_0(M_{h^\pm}^2, M_\mu^2) + dB_1(M_{h^\pm}^2, M_\mu^2)] \\
& + \frac{f_{\mathcal{R}} M_\mu v \mathcal{C}_{\mathcal{R}le}}{4\sqrt{2}\pi^2 \Lambda^2} [B_0(M_\mu^2, M_{r^{\pm\pm}}^2) + B_1(M_\mu^2, M_{r^{\pm\pm}}^2) + 2M_\mu^2 dB_0(M_\mu^2, M_{r^{\pm\pm}}^2)] \\
& + \frac{f_{\mathcal{S}} M_\mu v \mathcal{C}_{\mathcal{S}le}}{4\sqrt{2}\pi^2 \Lambda^2} [B_0(M_\mu^2, M_{r^{\pm\pm}}^2) + B_1(M_\mu^2, M_{r^{\pm\pm}}^2) + 2M_\mu^2 (dB_0(M_\mu^2, M_{r^{\pm\pm}}^2) + dB_1(M_\mu^2, M_{r^{\pm\pm}}^2))]. \tag{B4}
\end{aligned}$$

The vev-renormalization term is computed from the tadpole RC δT as $\delta v = -\delta T/M_H^2$ (see, e.g., [50]),

$$\begin{aligned} \delta v = & -\frac{1}{M_H^2} \left[\frac{g_W^2 M_W^2 v}{16\pi^2} + \frac{(g_Y^2 + g_W^2) M_Z^2 v}{32\pi^2} + \sum_{l=e,\mu,\tau} \frac{M_l^2 A_0(M_l^2)}{4\pi^2 v} + \sum_{q_u=u,c,t} \frac{3M_{q_u}^2 A_0(M_{q_u}^2)}{4\pi^2 v} + \sum_{q_d=d,s,b} \frac{3M_{q_d}^2 A_0(M_{q_d}^2)}{4\pi^2 v} \right. \\ & - \frac{3\lambda_1 v A_0(M_H^2)}{16\pi^2} - \frac{v(\lambda_5 A_0(M_{r^{\pm\pm}}^2) + \lambda_4 A_0(M_{h^\pm}^2))}{16\pi^2} - \frac{3g_W^2 v A_0(M_W^2)}{32\pi^2} - \frac{\lambda_1 v (2A_0(M_W^2) + A_0(M_Z^2))}{16\pi^2} \\ & - \frac{3(g_Y^2 + g_W^2) v A_0(M_Z^2)}{64\pi^2} + \frac{C_{\phi\mathcal{R}D}}{\Lambda^2} \left(\frac{M_{r^{\pm\pm}} v}{16\pi^2} + \frac{\lambda_5 v^3}{32\pi^2} \right) A_0(M_{r^{\pm\pm}}^2) + \frac{C_{\phi\mathcal{S}D}}{\Lambda^2} \left(\frac{M_{h^\pm} v}{16\pi^2} + \frac{\lambda_4 v^3}{32\pi^2} \right) A_0(M_{h^\pm}^2) \\ & \left. + \frac{C_{\phi\mathcal{R}} v^3 A_0(M_{r^{\pm\pm}}^2)}{\Lambda^2} + \frac{C_{\phi\mathcal{S}} v^3 A_0(M_{h^\pm}^2)}{\Lambda^2} \right]. \end{aligned} \quad (\text{B5})$$

The divergences associated with the Wilson coefficients are removed through $\overline{\text{MS}}$ renormalization of C_{eA} ,

$$\begin{aligned} \delta C_{eA} = & \left[\frac{f_S^2}{32\pi^2} + \frac{f_R^2}{16\pi^2} + \frac{g_W^2}{64\pi^2} + \frac{5g_Y^4}{128(g_Y^2 + g_W^2)\pi^2} + \frac{65g_Y^2 g_W^2}{192(g_Y^2 + g_W^2)\pi^2} + \frac{g_W^4}{128(g_Y^2 + g_W^2)\pi^2} - \frac{3\lambda_1}{16\pi^2} - \frac{\lambda_1 M_W^2}{8M_H^2 \pi^2} \right. \\ & - \frac{\lambda_1 M_Z^2}{16M_H^2 \pi^2} - \frac{(\lambda_5 M_{r^{\pm\pm}}^2 + \lambda_4 M_{h^\pm}^2)}{16M_H^2 \pi^2} - \frac{3g_W^2 M_W^2}{32M_H^2 \pi^2} - \frac{3(g_Y^2 + g_W^2) M_Z^2}{64M_H^2 \pi^2} - \sum_{l=e,\mu,\tau} \frac{M_l^4}{4M_H^2 \pi^2 v^2} - \sum_{q_u=u,c,t} \frac{M_{q_u}^4}{4M_H^2 \pi^2 v^2} \\ & \left. - \sum_{q_d=d,s,b} \frac{M_{q_d}^4}{4M_H^2 \pi^2 v^2} \right] \frac{C_{eA}}{\Lambda^2} + \left[\frac{g_Y g_W^3 M_W^2}{8(g_Y^2 + g_W^2) M_Z^2 \pi^2} + \frac{g_Y^3 g_W^3 v^2}{32(g_Y^2 + g_W^2) M_Z^2 \pi^2} \right] \frac{C_{eZ}}{\Lambda^2} + \frac{f_S M_\mu}{32\sqrt{g_Y^2 + g_W^2} \pi^2 v} \left(g_Y \frac{C_{eWS}}{\Lambda^2} + 2g_W \frac{C_{eBS}}{\Lambda^2} \right). \end{aligned} \quad (\text{B6})$$

2. Higgs decay

In this section, we have listed the renormalization constants (RC) computed for the case of 125 GeV Higgs decay to diphoton mentioned in Sec. III B. Here, we only mention the part of the RCs which arise due to the divergence coming through the coupling of $r^{\pm\pm}$ to other fields. The parts of the RCs containing the singly charged field h^\pm have been documented in the Appendix of Ref. [67]. The on-shell wave function RCs for the external fields are given as

$$\delta Z_{AA,r^{\pm\pm}} = \frac{g_Y^2 g_W^2 dB_{00}(M_{r^{\pm\pm}}^2)}{\pi^2 (g_Y^2 + g_W^2)} - \frac{A_0(M_{r^{\pm\pm}}^2) (C_{B\mathcal{R}} g_W^2 + C_{W\mathcal{R}} g_Y^2)}{4\pi^2 (g_Y^2 + g_W^2) \Lambda^2}, \quad (\text{B7})$$

$$\delta Z_{ZA,r^{\pm\pm}} = \frac{g_Y g_W (g_Y^2 B_{00}(M_{r^{\pm\pm}}^2) - g_Y^2 A_0(M_{r^{\pm\pm}}^2))}{\pi^2 M_Z^2 (g_Y^2 + g_W^2) \Lambda^2}, \quad (\text{B8})$$

and

$$\begin{aligned} \delta Z_{H,r^{\pm\pm}} = & \frac{1}{64\pi^2 \Lambda^2} (4C_{\phi\mathcal{R}D} \lambda_5^2 v^4 dB_0(M_H^2, M_{r^{\pm\pm}}^2) + 8C_{\phi\mathcal{R}} \lambda_5 v^4 dB_0(M_H^2, M_{r^{\pm\pm}}^2) + 8v^2 C_{\phi\mathcal{R}D} \lambda_5 B_1(M_H^2, M_{r^{\pm\pm}}^2) \\ & + 8C_{\phi\mathcal{R}D} \lambda_5 M_{r^{\pm\pm}}^2 v^2 dB_0(M_H^2, M_{r^{\pm\pm}}^2) + 8C_{\phi\mathcal{R}D} \lambda_5 M_H^2 v^2 dB_1(M_H^2, M_{r^{\pm\pm}}^2) + 4C_{\mathcal{R}\phi D} A_0(M_{r^{\pm\pm}}^2)). \end{aligned} \quad (\text{B9})$$

The tadpole counterterm is also computed in a similar fashion as given in Sec. B 1,

$$\delta v_{r^{\pm\pm}} = -\frac{A_0(M_{r^{\pm\pm}}^2)}{64\pi^2 M_H^2 \Lambda^2} (4v^3 C_{\phi\mathcal{R}} + 2\lambda_5 v^2 C_{\phi\mathcal{R}D} + 4M_{r^{\pm\pm}}^2 C_{\phi\mathcal{R}D} - 4v\lambda_5 \Lambda^2). \quad (\text{B10})$$

The RCs associated with the Wilson coefficients are given by

$$\delta\mathcal{C}_{A\phi,r^{\pm\pm}} = \frac{\lambda_5(g_Y^2\mathcal{C}_{WR} + g_W^2\mathcal{C}_{BR})}{16(g_Y^2 + g_W^2)\pi^2\Lambda^2}, \quad (\text{B11})$$

and

$$\delta\mathcal{C}_{\tilde{A}\phi,r^{\pm\pm}} = \frac{\lambda_5(g_Y^2\mathcal{C}_{\tilde{W}R} + g_W^2\mathcal{C}_{\tilde{B}R})}{16(g_Y^2 + g_W^2)\pi^2\Lambda^2}. \quad (\text{B12})$$

APPENDIX C: SINGLY CHARGED SCALAR CONTRIBUTION TO a_μ

As discussed in Sec. III A, the EFT scenario considered here plays an important role in explaining the observed measurement for a_μ , considering the effect of new propagating singly and doubly charged scalar fields. The effective dimension-6 contribution to a_μ from $r^{\pm\pm}$ is given in Eq. (15). The contribution to a_μ from h^\pm can be obtained after renormalizing the SMEFT structure shown in Eq. (10). For vanishing SMEFT Wilson coefficients, we can find the following form for a_μ contribution from dimension-6 effective h^\pm interactions:

$$\begin{aligned} \Lambda^2 \times a_\mu^{\text{d6},h^\pm} (\text{Zee-Babu}) &= \frac{f_S M_\mu^3 v (\mathcal{C}_{Ste})_{e\mu}}{24\sqrt{2}\pi^2 M_{h^\pm}^2} + \frac{f_S M_\mu^2 v^2 (\mathcal{C}_{l\phi S})_{e\mu}}{48\pi^2 M_{h^\pm}^2} + \frac{f_S^2 M_\mu^2 v^2 \mathcal{C}_{\phi SD}}{48\pi^2 M_{h^\pm}^2} \\ &+ \frac{f_S M_\mu^2}{8g_Y \pi^2} ((\mathcal{C}_{eBS})_{e\mu} + (\mathcal{C}_{eBS})_{\mu e}) \left[1 + \frac{2}{3} \left(\frac{M_\mu^2}{M_{h^\pm}^2} \right) + 2 \log \left(\frac{M_\mu^2}{M_{h^\pm}^2} \right) \right] \\ &- \frac{f_S M_\mu^2}{8g_W \pi^2} ((\mathcal{C}_{eWS})_{e\mu} - (\mathcal{C}_{eWS})_{\mu e}) \left[1 + \frac{2}{3} \left(\frac{M_\mu^2}{M_{h^\pm}^2} \right) + 2 \log \left(\frac{M_\mu^2}{M_{h^\pm}^2} \right) \right]. \end{aligned} \quad (\text{C1})$$

Due to the antisymmetric structure of f_S , $\mu \rightarrow \mu\gamma$ can proceed to happen via $\{\mu^\pm, \nu_e, h^\mp\}$ or $\{\mu^\pm, \nu_e, h^\mp, \gamma\}$ vertices, as shown in Fig. 7. As a result, these receive modifications from specific off-diagonal elements of contributing effective

operators in flavor space and the corresponding Wilson coefficients appear to contribute to a_μ , as can be seen in Eq. (C1). The covariant structures of the operators (\mathcal{O}_i) for the Wilson coefficients (\mathcal{C}_i) are given in Table I.

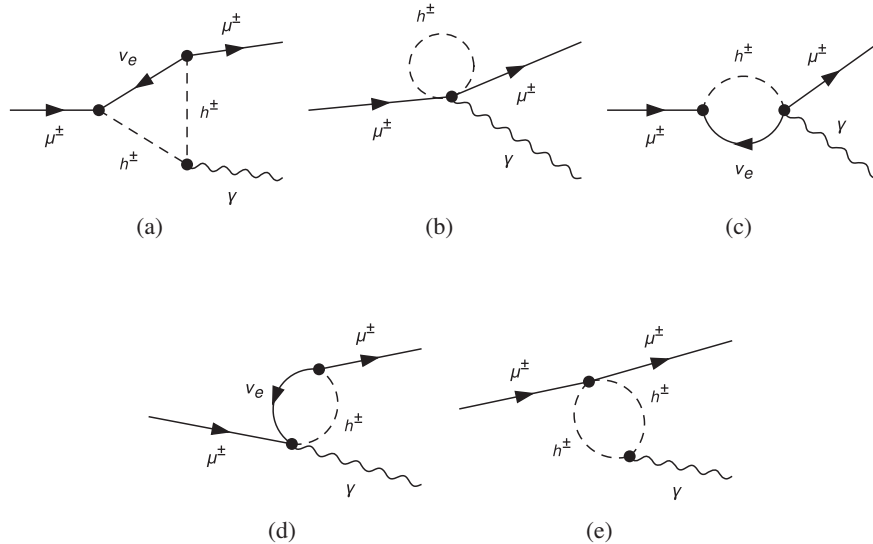


FIG. 7. BSM Feynman diagrams contributing to the muon anomalous magnetic moment $\mu \rightarrow \mu\gamma$ via h^\pm and its EFT interactions. The vertices include the renormalizable and the dimension-6 interactions.

- [1] B. Abi *et al.* (Muon $g-2$ Collaboration), *Phys. Rev. Lett.* **126**, 141801 (2021).
- [2] G. W. Bennett *et al.* (Muon $g-2$ Collaboration), *Phys. Rev. Lett.* **92**, 161802 (2004).
- [3] T. Aoyama, M. Hayakawa, T. Kinoshita, and M. Nio, *Phys. Rev. Lett.* **109**, 111808 (2012).
- [4] T. Aoyama, T. Kinoshita, and M. Nio, *Atoms* **7**, 28 (2019).
- [5] A. Czarnecki, W. J. Marciano, and A. Vainshtein, *Phys. Rev. D* **67**, 073006 (2003); **73**, 119901(E) (2006).
- [6] C. Gnendiger, D. Stöckinger, and H. Stöckinger-Kim, *Phys. Rev. D* **88**, 053005 (2013).
- [7] M. Davier, A. Hoecker, B. Malaescu, and Z. Zhang, *Eur. Phys. J. C* **77**, 827 (2017).
- [8] A. Keshavarzi, D. Nomura, and T. Teubner, *Phys. Rev. D* **97**, 114025 (2018).
- [9] G. Colangelo, M. Hoferichter, and P. Stoffer, *J. High Energy Phys.* **02** (2019) 006.
- [10] M. Hoferichter, B.-L. Hoid, and B. Kubis, *J. High Energy Phys.* **08** (2019) 137.
- [11] M. Davier, A. Hoecker, B. Malaescu, and Z. Zhang, *Eur. Phys. J. C* **80**, 241 (2020); **80**, 410(E) (2020).
- [12] A. Keshavarzi, D. Nomura, and T. Teubner, *Phys. Rev. D* **101**, 014029 (2020).
- [13] A. Kurz, T. Liu, P. Marquard, and M. Steinhauser, *Phys. Lett. B* **734**, 144 (2014).
- [14] K. Melnikov and A. Vainshtein, *Phys. Rev. D* **70**, 113006 (2004).
- [15] P. Masjuan and P. Sanchez-Puertas, *Phys. Rev. D* **95**, 054026 (2017).
- [16] G. Colangelo, M. Hoferichter, M. Procura, and P. Stoffer, *J. High Energy Phys.* **04** (2017) 161.
- [17] M. Hoferichter, B.-L. Hoid, B. Kubis, S. Leupold, and S. P. Schneider, *J. High Energy Phys.* **10** (2018) 141.
- [18] A. Gérardin, H. B. Meyer, and A. Nyffeler, *Phys. Rev. D* **100**, 034520 (2019).
- [19] J. Bijnens, N. Hermansson-Truedsson, and A. Rodríguez-Sánchez, *Phys. Lett. B* **798**, 134994 (2019).
- [20] G. Colangelo, F. Hagelstein, M. Hoferichter, L. Laub, and P. Stoffer, *J. High Energy Phys.* **03** (2020) 101.
- [21] T. Blum, N. Christ, M. Hayakawa, T. Izubuchi, L. Jin, C. Jung, and C. Lehner, *Phys. Rev. Lett.* **124**, 132002 (2020).
- [22] G. Colangelo, M. Hoferichter, A. Nyffeler, M. Passera, and P. Stoffer, *Phys. Lett. B* **735**, 90 (2014).
- [23] T. Aoyama *et al.*, *Phys. Rep.* **887**, 1 (2020).
- [24] G. Cowan, [arXiv:2107.02652](https://arxiv.org/abs/2107.02652).
- [25] H. Baer, V. Barger, and H. Serce, *Phys. Lett. B* **820**, 136480 (2021).
- [26] P. Athron, C. Balázs, D. H. Jacob, W. Kotlarski, D. Stöckinger, and H. Stöckinger-Kim, *J. High Energy Phys.* **09** (2021) 080.
- [27] M. Frank, Y. Hiçiyılmaz, S. Mondal, O. Özdal, and C. S. Ün, *J. High Energy Phys.* **10** (2021) 063.
- [28] J. Ellis, J. L. Evans, N. Nagata, D. V. Nanopoulos, and K. A. Olive, [arXiv:2107.03025](https://arxiv.org/abs/2107.03025).
- [29] D. Zhang, *J. High Energy Phys.* **07** (2021) 069.
- [30] A. Jueid, J. Kim, S. Lee, and J. Song, *Phys. Rev. D* **104**, 095008 (2021).
- [31] W. Altmannshofer, S. A. Gadam, S. Gori, and N. Hamer, *J. High Energy Phys.* **07** (2021) 118.
- [32] M. Chakraborti, S. Heinemeyer, and I. Saha, [arXiv:2105.06408](https://arxiv.org/abs/2105.06408).
- [33] M. Chakraborti, S. Heinemeyer, and I. Saha, [arXiv:2104.03287](https://arxiv.org/abs/2104.03287).
- [34] A. Zee, *Nucl. Phys.* **B264**, 99 (1986).
- [35] K. S. Babu, *Phys. Lett. B* **203**, 132 (1988).
- [36] H. Okada, T. Toma, and K. Yagyu, *Phys. Rev. D* **90**, 095005 (2014).
- [37] J. P. Leveille, *Nucl. Phys.* **B137**, 63 (1978).
- [38] S. R. Moore, K. Whisnant, and B.-L. Young, *Phys. Rev. D* **31**, 105 (1985).
- [39] M. Nebot, J. F. Oliver, D. Palao, and A. Santamaria, *Phys. Rev. D* **77**, 093013 (2008).
- [40] D. Schmidt, T. Schwetz, and H. Zhang, *Nucl. Phys.* **B885**, 524 (2014).
- [41] A. Crivellin, M. Ghezzi, L. Panizzi, G. M. Pruna, and A. Signer, *Phys. Rev. D* **99**, 035004 (2019).
- [42] B. Grzadkowski, M. Iskrzynski, M. Misiak, and J. Rosiek, *J. High Energy Phys.* **10** (2010) 085.
- [43] J. Aebischer, W. Dekens, E. E. Jenkins, A. V. Manohar, D. Sengupta, and P. Stoffer, *J. High Energy Phys.* **07** (2021) 107.
- [44] L. Allwicher, L. Di Luzio, M. Fedele, F. Mescia, and M. Nardecchia, *Phys. Rev. D* **104**, 055035 (2021).
- [45] J. Herrero-Garcia, M. Nebot, N. Rius, and A. Santamaria, *Nucl. Phys.* **B885**, 542 (2014).
- [46] S. F. King, A. Merle, and L. Panizzi, *J. High Energy Phys.* **11** (2014) 124.
- [47] I. Brivio, Y. Jiang, and M. Trott, *J. High Energy Phys.* **12** (2017) 070.
- [48] A. Dedes, W. Materkowska, M. Paraskevas, J. Rosiek, and K. Suxho, *J. High Energy Phys.* **06** (2017) 143.
- [49] A. Denner, *Fortschr. Phys.* **41**, 307 (1993).
- [50] A. Denner and S. Dittmaier, *Phys. Rep.* **864**, 1 (2020).
- [51] T. Hahn, *Comput. Phys. Commun.* **140**, 418 (2001).
- [52] T. Hahn and M. Perez-Victoria, *Comput. Phys. Commun.* **118**, 153 (1999).
- [53] H. H. Patel, *Comput. Phys. Commun.* **197**, 276 (2015).
- [54] G. Passarino and M. J. G. Veltman, *Nucl. Phys.* **B160**, 151 (1979).
- [55] J. S. Schwinger, *Phys. Rev.* **73**, 416 (1948).
- [56] O. Atkinson, M. Black, A. Lenz, A. Rusov, and J. Wynne, [arXiv:2107.05650](https://arxiv.org/abs/2107.05650).
- [57] A. Cherchiglia, P. Kneschke, D. Stöckinger, and H. Stöckinger-Kim, *J. High Energy Phys.* **01** (2017) 007.
- [58] P. Athron, C. Balázs, A. Cherchiglia, D. H. J. Jacob, D. Stöckinger, H. Stöckinger-Kim, and A. Voigt, [arXiv:2110.13238](https://arxiv.org/abs/2110.13238).
- [59] S. Dittmaier *et al.* (LHC Higgs Cross Section Working Group), [arXiv:1101.0593](https://arxiv.org/abs/1101.0593).
- [60] H. M. Georgi, S. L. Glashow, M. E. Machacek, and D. V. Nanopoulos, *Phys. Rev. Lett.* **40**, 692 (1978).
- [61] S. Dawson, *Nucl. Phys.* **B359**, 283 (1991).
- [62] A. Djouadi, M. Spira, and P. M. Zerwas, *Phys. Lett. B* **264**, 440 (1991).
- [63] A. M. Sirunyan *et al.* (CMS Collaboration), Report No. CMS-PAS-FTR-16-002.
- [64] J. de Blas *et al.*, *J. High Energy Phys.* **01** (2020) 139.
- [65] G. Aad *et al.* (ATLAS Collaboration), *Phys. Lett. B* **809**, 135754 (2020).
- [66] A. Djouadi, *Phys. Rep.* **457**, 1 (2008).

- [67] Anisha, U. Banerjee, J. Chakraborty, C. Englert, and M. Spannowsky, *Phys. Rev. D* **103**, 096009 (2021).
- [68] E. Boos and I. Volobuev, *Phys. Rev. D* **97**, 095014 (2018).
- [69] E. Bergeaas Kuutmann (ATLAS Collaboration), *Proc. Sci. EPS-HEP2017* (2017) 260.
- [70] T. Han, B. Mukhopadhyaya, Z. Si, and K. Wang, *Phys. Rev. D* **76**, 075013 (2007).
- [71] N. D. Christensen and C. Duhr, *Comput. Phys. Commun.* **180**, 1614 (2009).
- [72] A. Alloul, N. D. Christensen, C. Degrande, C. Duhr, and B. Fuks, *Comput. Phys. Commun.* **185**, 2250 (2014).
- [73] C. Degrande, C. Duhr, B. Fuks, D. Grellscheid, O. Mattelaer, and T. Reiter, *Comput. Phys. Commun.* **183**, 1201 (2012).
- [74] J. Alwall, R. Frederix, S. Frixione, V. Hirschi, F. Maltoni, O. Mattelaer, H. S. Shao, T. Stelzer, P. Torrielli, and M. Zaro, *J. High Energy Phys.* 07 (2014) 079.
- [75] J. Alwall, M. Herquet, F. Maltoni, O. Mattelaer, and T. Stelzer, *J. High Energy Phys.* 06 (2011) 128.
- [76] P. de Aquino, W. Link, F. Maltoni, O. Mattelaer, and T. Stelzer, *Comput. Phys. Commun.* **183**, 2254 (2012).
- [77] J. Alwall, C. Duhr, B. Fuks, O. Mattelaer, D. G. Öztürk, and C.-H. Shen, *Comput. Phys. Commun.* **197**, 312 (2015).
- [78] M. Aaboud *et al.* (ATLAS Collaboration), *Eur. Phys. J. C* **78**, 199 (2018).
- [79] G. Altarelli, R. K. Ellis, and G. Martinelli, *Nucl. Phys.* **B157**, 461 (1979).
- [80] U. Banerjee, J. Chakraborty, S. Prakash, S. U. Rahaman, and M. Spannowsky, *J. High Energy Phys.* 01 (2021) 028.
- [81] U. Banerjee, J. Chakraborty, S. Prakash, and S. U. Rahaman, *Eur. Phys. J. C* **80**, 938 (2020).